Biotic and Environmental Fluctuations during Permian-Triassic transition: A Biomarker and Stable Isotope Approach

Vasudev

MS14040

A dissertation submitted for the partial fulfilment of BS-MS dual degree in Science

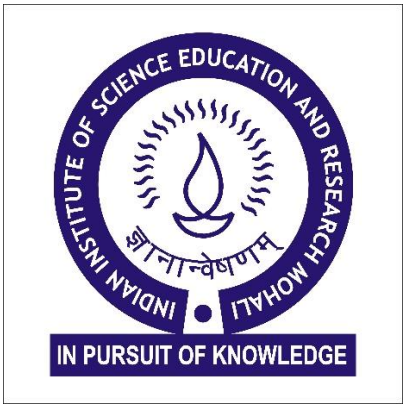

Indian Institute of Science Education and Research Mohali

April, 2019

Certificate of Examination

This is to certify that the dissertation titled "Biotic and Environmental Fluctuations during Permian-Triassic transition: A Biomarker and Stable Isotope Approach" submitted by Vasudev (MS14040) for the partial fulfilment of BS-MS dual degree programme of the Institute, has been examined by the thesis committee duly appointed by the institute. The committee finds the work done by the candidate satisfactory and recommends that the report be accepted.

Dr. Sunil Patil Dr. Anoop Ambili Dr. Sharmila Bhattacharya

Thesis Supervisor

Date: April 26, 2019

Declaration

The work presented in this dissertation has been carried out by me under the guidance of Dr. Sharmila Bhattacharya at the Indian Institute of Science Education and Research Mohali. This work has not been submitted in part or in full for a degree, a diploma, or a fellowship to any other university or institute. Whenever contribution of others are involved, every effort is made to indicate this clearly, with due acknowledgement of collaborative research and discussions. This thesis is a bona fide record of original work done by me and all sources listed within have been detailed in the bibliography.

Vasudev

Date: April 26, 2019

In my capacity as the supervisor of the candidate's project work, I certify that the above statements by the candidate are true to the best of my knowledge.

Dr. Sharmila Bhattacharya

Thesis Supervisor

Acknowledgements

I am greatly thankful to my thesis supervisor Dr Sharmila Bhattacharya, Inspire Faculty, Department of Earth & Environmental Sciences, Indian Institute of Science Education and Research Mohali India, for her continuous encouragement and valuable guidance to complete my thesis work. My grateful thanks are due for her support throughout my thesis, her patience and knowledge whilst allowing me the room to work in my own way. Without her this thesis would not have been completed. Her approach, vision, hard work and guidance in research enabled me to learn a lot.

I express my profuse and heartfelt thanks to Dr Anoop Ambili, Assistant Professor, Department of Earth & Environmental Sciences, Indian Institute of Science Education and Research Mohali India, for his precious suggestions that helped me to improve my thesis work. I thank him for his suggestions and guidance at every stage of my research work.

Thanks are due to the members of PRISM lab for their help with data acquisition and interpretation. I wish to extend my warmest thanks to Ankit (PhD, IISER, Mohali), Bulbul (PhD, IISER, Mohali), Dipti (PhD, IISER, Mohali), Sunil (PhD, IISER, Mohali), Parth (PhD, University of Haifa, Israel) and Muneer (PhD, Kashmir University) who helped me with my work in the lab.

I would also acknowledge Vishal Kumar Porwal, Sushmita Nahar and Vishal Kumar Sharma for their willingness to help and discuss important ideas relevant to my work. To my friends and colleagues, thank you for listening, offering me advice, and supporting me through this entire process. Thank you for your thoughts, well-wishes, phone calls, e-mails, texts, visits, and being there whenever I needed a friend.

I express my deep sense of gratitude to my beloved Parents and my younger brother for their inseparable support and prayers. My Father, Mr Satyawan Singh, in the first place is the person who put the seeds of my learning character, showing me the joy of intellectual pursuit ever since I was a child. My Mother, Mrs Rajesh Rani, is the one who sincerely raised me with her caring and love.

Thanks for all your encouragement!

Contents

List of Figures

Figure 16: The Buchi E-914 Speed Extractor used for bitumen extraction.

Figure 17: The asphaltene fraction settled at the bottom of the beaker and the supernatant maltene fraction.

Figure 18: Photograph showing the silica gel column chromatography technique for the separation of different (saturated, aromatic and polar) hydrocarbon fractions.

Figure 19: Photograph of GC-MS facility at PRISM Lab, IISER Mohali.

Figure 20: The normal alkanes distribution in the selected ion chromatogram at *m/z* 57 in the saturated hydrocarbon fraction of Permian (RB/M/4X/64 and RB/M/4X/69) and Triassic (RB/M/4X/47 and RB/M/4X/19) continental sediments from Raniganj sub-basin showing a shift in the dominant chain lengths.

Figure 21: The shift in the *n*-alkane chain length distributions across the Permian-Triassic boundary recorded from continental sediments from Raniganj sub-basin.

Figure 22: Structure of chlorophyll showing the phytyl chain length attached to the porphyrin ring. Pristane and phytane are diagenetically altered products of phytyl chain in oxidising and reducing conditions, respectively.

Figure 23: The shift in the pristine/phytane ratio across the Permian- Triassic boundary recorded from continental sediments from Raniganj sub-basin.

Figure 24: Selected ion chromatogram at *m/z* 191 showing the relative abundance of hopanes in the saturated hydrocarbon fraction of Permian (RB/M/4X/32), P/T boundary (RB/M/4X/58) and Triassic (RB/M/4X/68) continental sediments from Raniganj sub-basin.

Figure 25: Selected ion chromatogram at *m/z* 245 showing the presence of *ent*-18-nor-16β(H)-kaurane in the saturated hydrocarbon fraction of Permian (RB/M/4X/68) and P/T boundary sediments (RB/M/4X/58); however, the compound is not detected in the Triassic sediment (RB/M/4X/41).

Figure 26: The carbon isotope record $\delta^{13}C_{bulk}$ showing a sharp excursion across the Permian-Triassic boundary recorded from continental sediments in Raniganj sub-basin.

List of Tables

Abstract

The Permian-Triassic transition qualifies as the severest mass extinction boundary the planet has so far witnessed. In the present study, we report geochemical analyses, viz. biomarker and stable isotope record of continental Permo-Triassic sediments from a core (=257 m) retrieved from a borehole located at Madhukunda, Raniganj sub-basin in West Bengal in an attempt to understand any biotic and palaeoenvironmental fluctuations accompanying the Permo-Triassic extinction event. The present study also documents field observations from the Gondwana Permo-Triassic sediments. Typical Permian Gondwana flora viz. *Glossopteris*, *Vertebraria* and *Equisetales* were found in the Permian Raniganj Formation; however, these were not observed in the Triassic rocks. The biomarker analysis was performed by extracting the soluble organic matter from the sediments in a speed extractor and fractionating the bitumen into saturated hydrocarbon fraction using silica gel chromatography. The saturated hydrocarbon fraction was analyzed using gas chromatography mass spectrometry (GC-MS). Pronounced shifts in the biomarker and stable isotopic composition were noteworthy. Normal alkanes which are derivatives of epicuticular waxes were recorded in the presently studied samples ranging in chain length from *n*-C_{16} to *n*-C_{31}. The normal alkane distribution was characterized by a predominance of *n*-C_{23} and *n*-C_{25} chain lengths in the Permian sediments which switched to a prevalence of *n*-C_{27} and *n*-C_{29} chain lengths in the Triassic sediments. A changeover is also reflected in the pristine-phytane (Pr/Ph) distribution which are acyclic isoprenoids derived from the phytyl side chain of chlorophyll wherein the Pr/Ph values decrease towards the Triassic sediments. These reflect a shift in the environmental conditions from an oxic, swampy, coal-forming environment during the Permian to drier conditions in the Triassic. Signatures of microbial reworking of the organic matter include the series of hopanes ranging from C_{27} to C_{32}. Trisnorneohopane (Ts) and trisnorhopane (Tm) are the dominant C_{27} hopanes detected. A marked decrease in the Ts and Tm concentrations has been noted for the Triassic sediments. Both αβ and βα stereoisomers of C_{30} hopanes were detected. 4β(H)-19-Norisopimarane, a tricyclic diterpane, was detected in low abundance in the Triassic samples whereas both tricyclic and tetracyclic diterpanes like *ent*-kaurane and phyllocladane were recorded from the Permian sediments reflecting the prevalence of broader diversity of gymnosperm flora during the Permian period.

CHAPTER 1

INTRODUCTION

1.1 BACKGROUND

The ledger of life on Earth demonstrates that mass extinction has been an inevitable, irreversible and possibly a cyclic phenomenon. Perhaps, it is a natural sieve mechanism wherein organisms that fail to cope up with the changing dynamics of the planet are eliminated. The wiping out of life on a massive scale from the face off the Earth has been observed multiple times (Raup and Sepkoski, 1982). The Earth, as we see today, is a far reaching outcome of two of the greatest organic events- the Cambrian explosion and the Permo-Triassic mass extinction since these played crucial roles in the design of the biosphere. The Earth had already witnessed five big mass extinctions and several small scale episodes of loss of life. Interestingly, three of the big five mass extinctions occurred during Palaeozoic (e.g. Peters, 2008). The end-Permian and its culmination into Triassic is marked by the severest biotic and ecosystem collapse in the history of Earth which decimated life on an unprecedented scale (Sepkoski, 1984; Erwin, 1994; Benton and Twitchett, 2003). The age of the end-Permian mass extinction was determined using single crystal zircon closed-system U-Pb dating to be 252.6 ± 0.2 Ma (Metcalfe and Isozaki, 2009). Further high precision U-Pb dating revealed that the extinction peak occurred at 252.28 ± 0.08 Ma (Shen et al., 2011). The planet witnessed the most pronounced global-scale state shift during the Permo-Triassic period (Barnosky et al., 2012) which had caused a complete restructuring of the biotic realm and is largely responsible for the design of the present biosphere (Chen and Benton, 2012). The global catastrophe was a hard blow to both marine and terrestrial ecosystems wherein 90% of species in the ocean and around 70% of vertebrates on land (Erwin, 1994) became extinct. The presence of Pangaea (Fig. 1) during Permian had been a windfall which facilitated the dispersal and spread of flora and fauna. However, the diversity and proliferation of the biosphere came to a halt with the "Great Dying" as the extinction phase is colloquially known. The ominous event ruined the Permian biosphere which had been teeming with life. Environmental perturbations are evident and have been demonstrated through negative $\delta^{13}C_{carb}$ and $\delta^{13}C_{org}$ excursions both in the marine and the terrestrial domains (Magaritz et al., 1988; de Wit et al., 2002; Ghosh et al., 2002; Cui et al., 2015). The catastrophic event also led to

geomorphic consequences inducing shift in river morphology from meandering to braided pattern due to removal of rooted plants (Ward et al., 2000). The coal-gap during Early Triassic and occurrences of rarefied coal deposits during Middle Triassic are aftermath caused by the extinction events and is recorded as a global phenomenon (Retallack et al., 1996). Correspondingly, there is a reef gap which is deemed as another effect of the extinction phenomenon (Flügel, 1994). The causal mechanism of the crisis has been inconclusive so far and synergistic combinations of phenomena may have led to the global perturbation. Many leading candidates that have been considered as triggers of the event are global scale anoxia (Wignall and Hallam, 1992; Wignall and Twitchett, 1996), euxinia (Grice et al., 2005; Cao et al., 2009), hypercapnia (Knoll et al., 1996), extreme high temperature of the oceans (Chen et al., 2013) and eruption of Siberian Traps leading to the release of massive quantities of green house gases (Svensen et al., 2009). Although the cause of extinction is still debated, the more acceptable notion is that of a synchronous disturbance in the marine and terrestrial realms that punctuated the Permian Triassic boundary (PTB) (Fenton et al., 2007; Nabbefeld et al., 2010; Shen et al., 2011).

The pattern of disappearance of organisms is complex and episodic rather than drastic or gradual (Erwin, 1994). Recent studies of marine records have revealed the possibility of two pulses of extinction (Song et al., 2013). The marine crisis was later reproduced on land wherein a large population was obliterated. The arthropod community experienced a huge decline and this is the only known mass extinction of insects (Chen and Benton, 2012). There are several established proxies for identifying Permian–Triassic mass extinction. *Hindeodus parvus*, a conodont index fossil, is considered as a marker for Permian–Triassic boundary (Yin et al., 2001). The chemical relicts and biogeochemical anomalies of the extinction event are also widespread and documented from several localities on Earth (Schwab and Spangenberg, 2004; Luo et al., 2013). The C_{33} *n*-alkylcyclohexane is considered as a marker for the extinction event possibly derived from some phytoplankton that evolved and proliferated during and immediately after the crisis event (Grice et al., 2005). The effect of mass extinction on plant community is patchy and a significant number of them survived complete demise (Hochuli et al., 2010). The transition phase in the terrestrial arena is well encoded in spores and pollens which indicate fungal proliferation and the shift of gymnosperm-dominated ecosystem to lycopod assemblages although

gymnosperms recovered during later stages. The crisis phase was followed by biotic recovery which occurred 4–5 Ma years later and interestingly the organisms that appeared were characterized by exceedingly small sizes regarded as the "Lilliput effect" (Twitchett, 2007). It took almost 10 Ma for the biological domain of the Earth to refurbish from the widespread killing event.

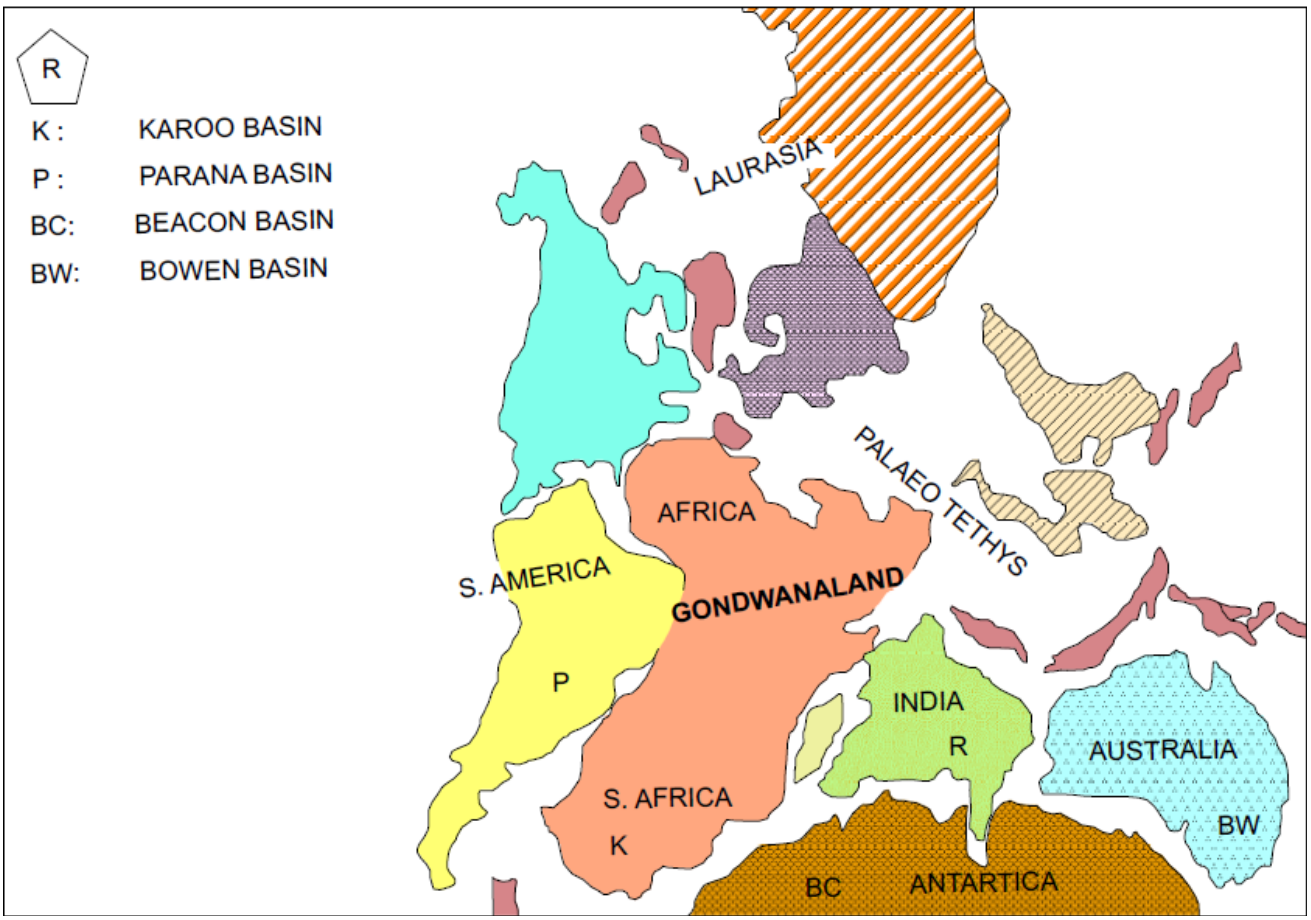

Figure 1: The supercontinent Pangea with the two components Laurasia and Gondwanaland and depicting the southern hemisphere continents preserving the Permian-Triassic sediments. Modified after Scotese (http://www.scotese.com/).

In the Indian context, marine Permo-Triassic sections are exposed in the extra-peninsular India (Guryul Ravine in Kashmir and in Spiti). The boundary in Spiti is easily identified by a reddish ferruginous band (Ghosh et al., 2002). Terrestrial sections are developed in the terrestrial Gondwana Basins of peninsular India such as Damodar, Satpura, South Rewa, Mahanadi,

Pranhita-Godavari and Rajmahal basins (Fig. 2). The Permian–Triassic successions, both marine and continental, were studied by some researchers (Sarkar et al., 2003; Algeo et al., 2007; Tewari et al., 2014; Ghosh et al., 2015). Sarkar et al. (2003) made some interesting observations (from terrestrial succession) like the significant depletion of $\delta^{13}C$ in slightly upper part of Triassic Panchet Formation (and not spot on at the P-T boundary) although depleted values, co-relatable with now widely separated regions like Australia and South Africa, at P-T boundary were also reported. Both Sarkar et al. (2003) and Algeo et al. (2007) have argued, based on isotopic analysis, that the causes of P-T extinction were Earth-bound and not triggered by some extra-terrestrial impact. The marine Guryul Ravine P-T section was studied by Tewari et al. (2014) and a marine palynostratigraphy was documented. The palynoassemblage comprises of relicts of fungi, algae and plant remains like spore, pollen and cuticles. Also, recent studies from the marine Spiti succession, India (Ghosh et al., 2016) put forward several probable causes of the extinction.

Hydrocarbon biomarkers derived from the macromolecules of past organisms upon burial and diagenesis are informative molecules that can reveal biodiversity, palaeoenvironment and evolutionary history of Earth in deep time (Brocks and Summons, 2003; Brocks and Pearson, 2005, Peters et al., 2005) (Fig. 3). Moreover, these provide information related to maturity and biodegradation of organic matter which are essential for the reconstruction of the geological processes occurring on the planet (Peters et al., 2005 and references therein). These are particularly important when there is a dearth of recognizable body or trace fossils. The labile fractions of organic matter viz. carbohydrates, proteins and nucleic acids are mostly recycled or degraded. However, the lipid portion is recalcitrant enough to successfully make its way into the geosphere on most occasions (Brocks and Summons, 2003).

The studies have, by and large, focused on Permo-Triassic marine fossil and terrestrial invertebrate records so far to understand the pulses of extinction. In contrast to the extensive perusal of Permo-Triassic marine and terrestrial vertebrate records, the studies on plant communities are equivocal. The aim of the present study is to scrutinize the late Permian- early Triassic turnover of vegetation and palaeoenvironment using a combination of biomarkers and

stable carbon and nitrogen isotope signatures in terrestrial succession from Gondwana Basin in India.

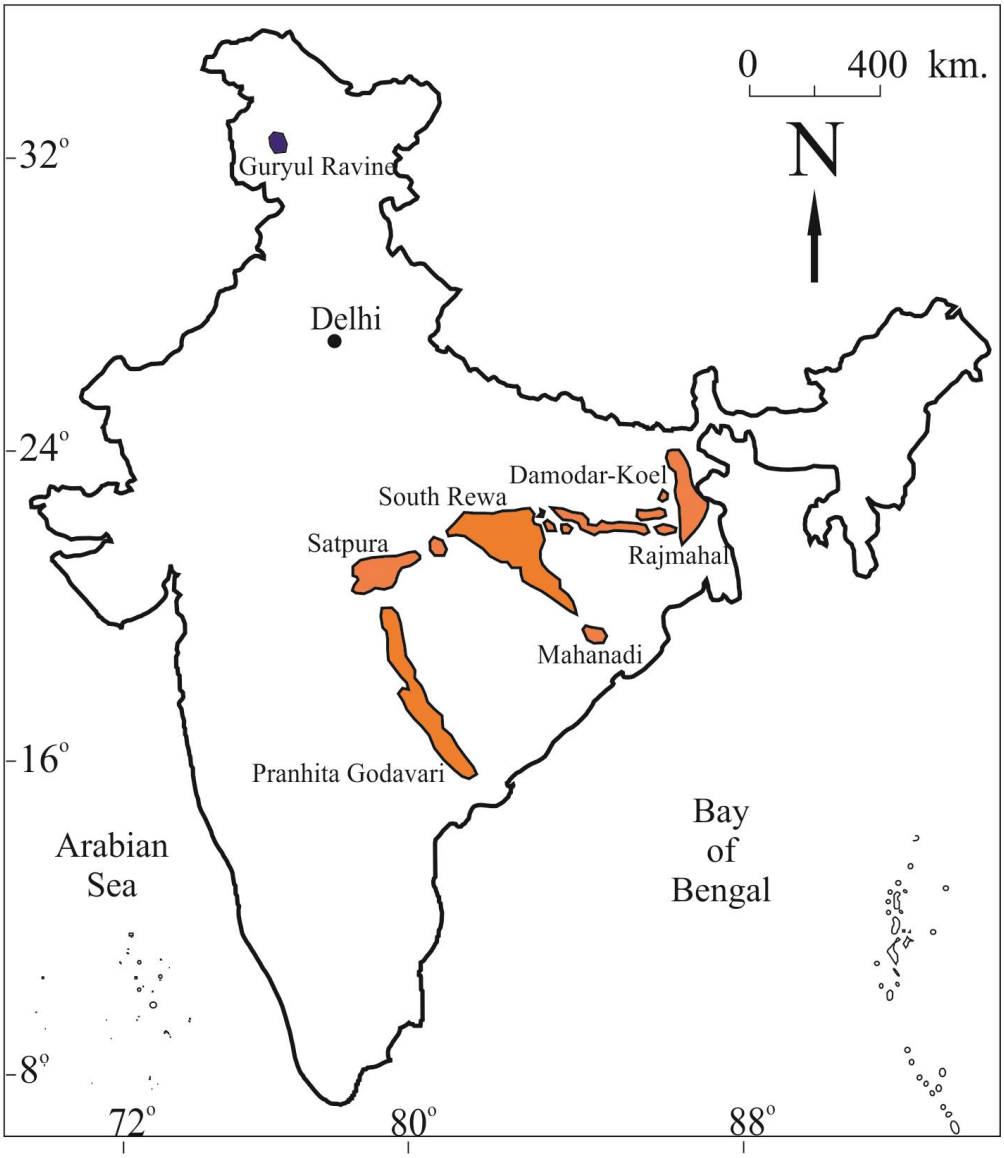

Figure 2: Gondwana basins preserving Permian-Triassic continental successions in peninsular India. Marine succession is exposed in the Guryul Ravine of Kashmir valley.

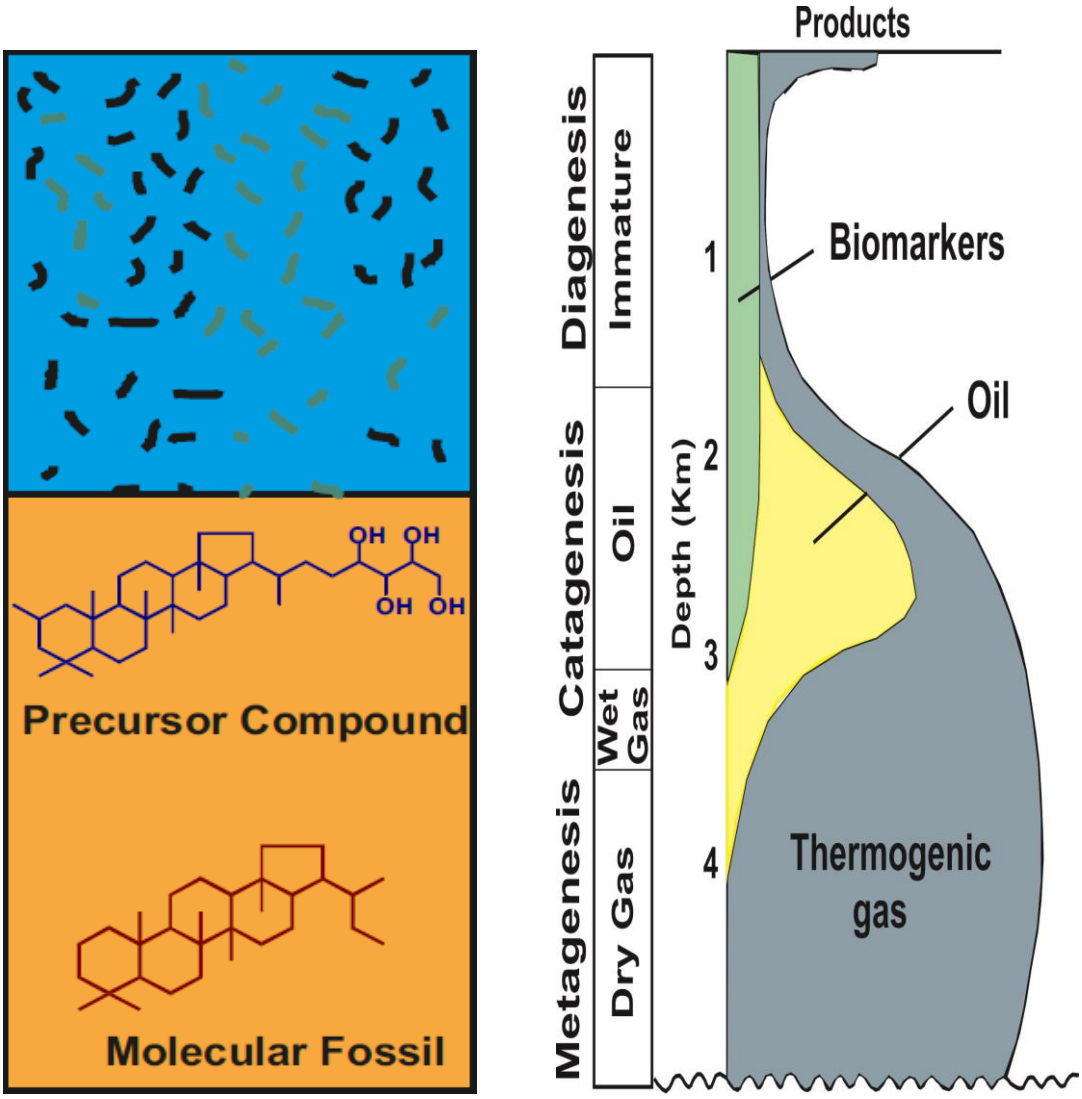

Figure 3: The formation of biomarkers in the geosphere derived from the macromolecules which in turn are released during cell lysis after the demise of organisms. The biomarkers are produced during diagenetic and catagenetic stages during the burial of organic matter.

1.2 OBJECTIVES

The present thesis addresses the following questions;

- Permo-Triassic mass extinction, in spite of being the severest organic cataclysm on the planet, is not very well understood.
- Fistful knowledge still exists for the marine P/T sections; however, the terrestrial P/T realm, which is a potential storehouse of geological information, is not well-studied.
- No comprehensive biomarker or compound specific isotope database exist for Permo-Triassic, particularly from Indian terrestrial successions.
- Understanding the duration, exact causal mechanism and complexities of the end-Permian extinction is cardinal to the reconstruction of the greatest mass extinction event on the planet.

Hence, the objectives of the present study are:

- Prepare a comprehensive database of Permian-Triassic biomarkers since these are informative molecules which can reveal a plethora of biological information such as biotic origin and signatures of metabolic activities.
- Probe the changeover of biomarkers (lipid constituents) and probable inception of new biosynthetic pathways.
- Reconstruction of the Permian-Triassic environmental conditions and palaeohabitat.

CHAPTER 2

STUDY AREA

2.1 GEOLOGICAL BACKGROUND OF THE STUDY AREA

Continental Permian and Triassic rocks occur in the Gondwana sedimentary basins in the eastern and central parts of the Indian peninsular craton (Ghosh, 2002). The Gondwana basins have a long history of sedimentation comprising both Lower Gondwana (Permian) and Upper Gondwana (Triassic–lower Cretaceous) formations which are predominantly silicilastic sediments (Mukhopadhyay et al., 2010). In the present study, borehole samples were collected from Madhukunda east, Raniganj Sub-basin (23°36´N, 86°52´E) which is the easternmost depository of the E-W to WNW-ESE trending Damodar basin (Gupta, 1999). The Raniganj Sub-basin is semi-elliptical and elongated in shape covering an area of about 3000 km^2. In the Damodar Basin, sedimentation commenced with the Talchir sediments followed by Karharbari, Barakar, Barren Measures and Raniganj Formations of Permian and Panchet Formation of Triassic. The Panchet Formation culminates to a long hiatus thereafter which the Jurassic Suprapanchet is encountered which is again followed by a sedimentary hiatus (Mukhopadhyay et al., 2010). Coal predominantly occurs at two stratigraphic sequences in the Early Permian Barakar and the Late Permian Raniganj formations. However, some coal seams are also associated with the Karharbari Formation.

The geological map with the location of the borehole of Raniganj Sub-basin is presented in Fig. 4 and the lithological sequences encountered in the borehole are presented in the form of a litholog in Fig. 5. In the present study, we have focused on the upper Permian Raniganj and the lower Triassic Panchet formations both of which were encountered in the studied borehole and recognized based on lithology. The Raniganj Formation comprises alternating layers of sandstone and shale with intermittent sandy shale, carbonaceous shale, coaly shale and coal. The Panchet Formation comprises alternating layers of thick sandstone layers and thin shale bands with intermittent sandy shale layers. The contact between the Raniganj and Panchet formations is marked by conglomerate lenses and thin mudstone/siltstone. The quintessential Gondwana flora

(*Glossopteris*) is observed in the late Permian Raniganj Formation which is clearly absent in the early Triassic Panchet Formation.

2.2 SAMPLING

Borehole samples (n=29) from a 257-m-thick section across the Permian-Triassic boundary were collected and investigated for the present study. The core samples were recovered from Madhukunda east, Raniganj sub-Basin from the location depicted in Fig. 4. The detailed lithology is provided in Fig. 5.

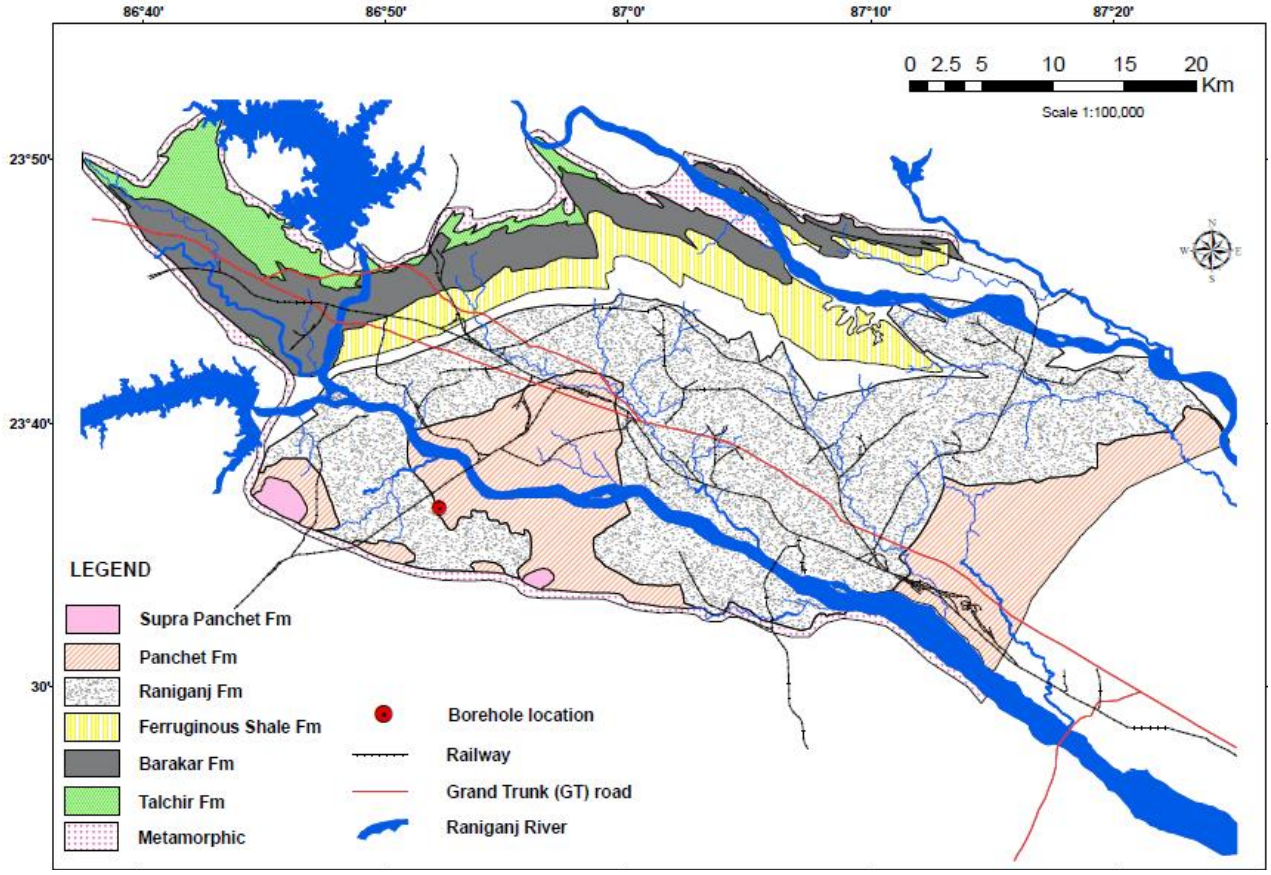

Figure 4: The geological map of the Raniganj Basin, West Bengal. The borehole location from which the studied core has been recovered is marked by a red solid circle.

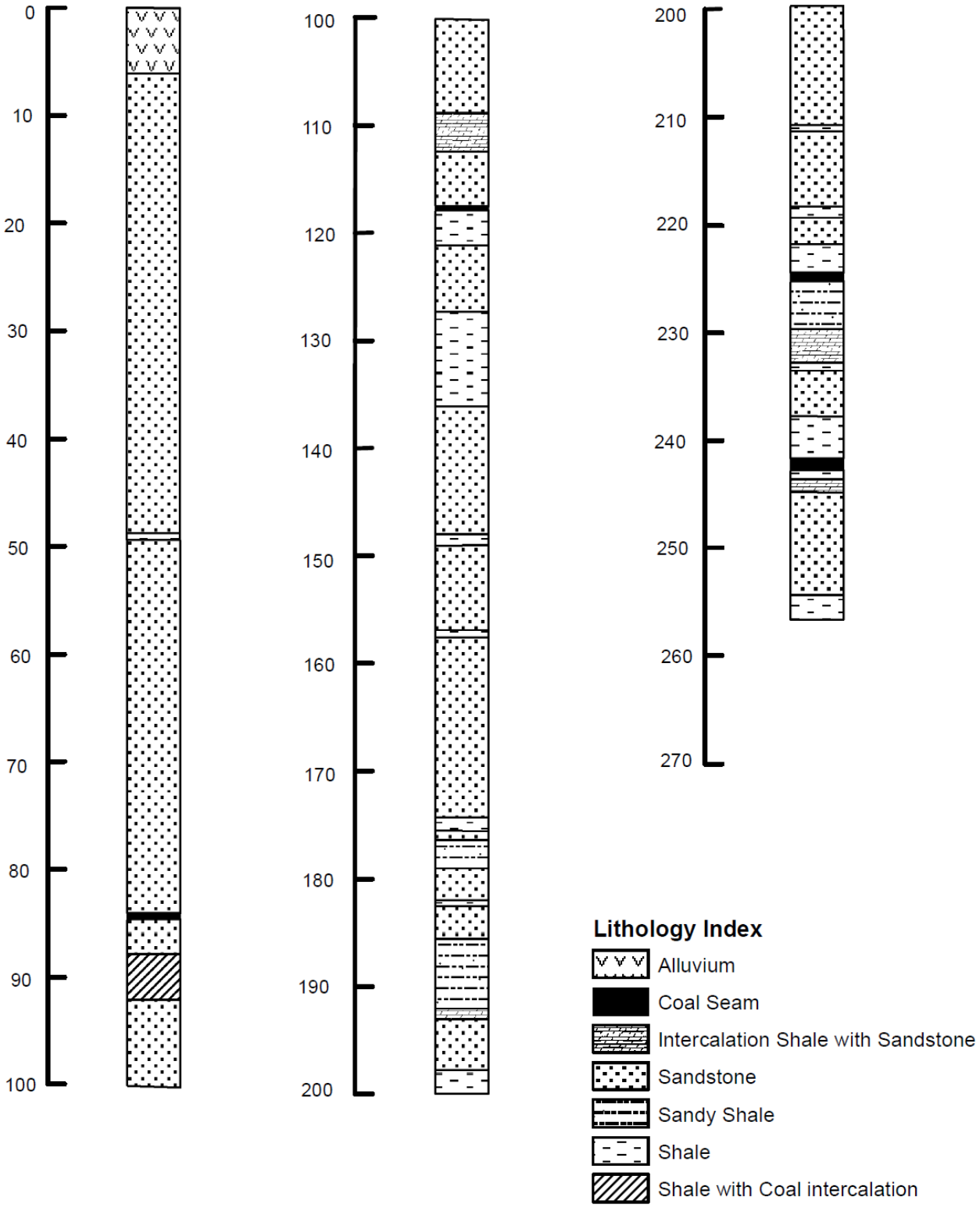

Figure 5: The detailed lithology of Panchet and Raniganj formations of the recovered core.

Figure 6: The borehole samples of Panchet and Raniganj Formations, Madhukunda. The retrieved core of 257 meters is placed in order from younger to older (left to right). The younger cores from Triassic are mostly sandstone, shale and mica rich rocks. The Permian rocks in the right comprise of shale, coaly shale and coal as well as sandstone.

Figure 7: The conglomerate layer at the P/T boundary in borehole section.

2.3 FIELD OBSERVATIONS

The uppermost Permian rocks are exposed along the Bagalgoria nala which is located at a distance of about 200 km WNW from Kolkata (Fig. 8). The sequences include a coal layer followed by sandstone, carbonaceous shale and sandstone. The Permian plant fossils viz. *Equisetales* (Fig. 9), *Vertebraria* (Fig. 10) and *Glossopteris* (Fig. 11) were encountered at the Bagalgoria nala area. These were the main floristic components of the Gondwana supercontinent during the Permian period that occurred in all the southern hemisphere continents. *Vertebraria* is considered as the underground rooted part of the glossopterids (Archangelsky, 1996). *Glossopteris* is one of the components of the Gondwana flora which formed a very distinctive late Palaeozoic and Mesozoic high latitude flora of the southern hemisphere different from the flora of the other Permian floristic provinces, viz. the Euramerican, Angara and Cathysian (McLoughlin, 2001 and references therein). The flora had been quite robust and tolerant which withstood the environmental perturbations of the end-Permian mass extinction and continued to survive into the Triassic although with reduced vigour and eventually succumbed to the end-Triassic extinction. *Glossopteris* palaeobiology is intricate since whole plant reconstruction has been achieved only with tiny pieces due to lack of intact preserved large portions. However, over the years, a wealth of information on *Glossopteris* have been garnered which have revealed few interesting aspects of this large woody plants. Detailed morphological and anatomical studies have revealed a gymnospermous affinity for the plant (McLoughlin, 2011). Most importantly, this distinctive flora attests the presence of Pangea and Wegener's continental drift theory on the basis of its presence on all the southern landmasses during the Permian, which are now widely separated from each other and hence a robust tool in palaeobiogeographic studies.

The boundary is marked by a matrix-supported conglomerate in the outcrop characterized by pebbly quartz and sandy and clayey matrix (Fig. 12). The presence of the conglomerate reflects shift in the sediment influx possibly influenced by the P/T extinction event wherein the megaflora of the terminal Permian were obliterated resulting in increased erosion of the river banks (Ward et al., 2000). The Triassic cross-bedded sandstone is exposed along Banspetalli nala (23°37´N, 86°54´E) (Fig. 13) and highly weathered Triassic shales are exposed near Dumdumi (Fig. 14).

Figure 8: Permian sequences at Bagalgoria nala, Madhukunda.

Figure 9: Fossil *Equisetales*, river section, Madhukunda.

Figure 10: Fossil *Vertebraria*, river section, Madhukunda.

Figure 11: *Glossopteris* fossils in shale, river section, Madhukunda.

Figure 12: The matrix supported conglomerate with pebble sized clasts indicating the boundary of the Panchet formation and Raniganj formation.

Figure 13: The cross-bedded Triassic Sandstone rocks encountered at a river section (Banspetalli Nala), Madhukunda.

Figure 14: Triassic Shale exposed near Dumdumi, Madhukunda.

CHAPTER 3

METHODOLOGY

3.1 TOC AND STABLE ISOTOPE ANALYSIS ($\delta^{13}C_{bulk}$)

Total 42 sedimentary rock samples were powdered to clay sized fraction using mortar and pestle. The stable isotope analysis for $\delta^{13}C$ requires the removal of inorganic carbon (TIC i.e. Total Inorganic Carbon) in form of carbonates from the powdered samples. To remove the carbonates from the samples, 1 gram of each sample was taken in 100 ml beakers and treated with 0.5 N hydrochloric acid (HCl). Sample with CO_2 effervescence were reported. The treated samples in HCl were kept in fume-hood for at least one day for complete carbonate removal. After the cessation of the effervescence, samples were centrifuged using Simran Laboratory Centrifuge at 4000 rpm to separate out the powdered samples and washed multiple times with double distilled water to clear away the HCl. The complete elimination of HCl was tested and ensured using pH paper. The wet samples were dried in oven at a temperature of 40°C. The dried samples were collected in 5 ml glass vials.

For isotope analyses, the powdered samples (~ 3-5 mg) were weighed and carefully packed into pre-combusted tin capsules. The sample filled tin capsules were introduced into the pre-filled and conditioned reactor of Elemental Analyzer (Flash EA 2000 HT) through an auto sampler. The CO_2 gas produced through the combustion was introduced into the Continuous Flow Isotope Ratio Mass Spectrometer (CFIRMS, MAT 253) coupled with Con-Flow IV interface for isotopic analysis (Fig. 15).

Repeat measurements were performed for all the samples to check the reproducibility. IAEA CH_3 (reported $\delta^{13}C$ value = $-$ 24.7 ‰) was used to calibrate the reference gas and carbon isotopic data has been reported against VPDB. International standards (CH_3 and CH_6) as well as internal standards (Sulfanilamide) were run to check the accuracy for the CO_2 measurements with an external precision of ±0.1‰ (1σ). All samples were analyzed at the Stable Isotope Laboratory, Birbal Sahni Institute of Palaeosciences (BSIP), Lucknow.

Figure 15: Photograph showing elemental analyzer (EA) coupled with Isotope ratio Mass spectrometer (IRMS).

3.2 BIOMARKER ANALYSIS USING GAS CHROMATOGRAPHY MASS SPECTROMETRY (GC-MS)

3.2.1 EXTRACTION OF BITUMEN FROM SEDIMENTS

The sedimentary rock samples were first powdered to sand sized using mortar and pestle. The amount of the samples taken for powdering ranged between 5 g to 100 g for different samples based on the Total Organic Carbon (TOC) content of these samples. The organic matter (bitumen) was extracted from the powdered samples using Buchi E-914 Speed Extractor (Fig. 16). For this, the powdered sample was first mixed with fat free, fire dried quartz sand (0.3 to 0.9) which is specifically used for the extraction purpose. The mixture was packed in clean extraction cells with all the standard techniques. The preheated (at 100°C) speed extractor was loaded with the extraction cells. Both the inlets were connected to the solution bottles (DCM and CH_3OH). The solution used for the extraction process was Methanol and Dichloromethane in 7:93 v/v ratios. The temperature and pressure were set at 100°C and 100 bar respectively. The number of extraction cycles performed on one sample was set at 2. After the extraction process

completed, the extract from the extraction bottles was collected in 250 ml clean beakers. The beakers were covered with aluminum foil and kept in the fume hood for drying.

Figure 16: The Buchi E-914 Speed Extractor used for bitumen extraction.

3.2.2 ASPHALTENE SEPARATION

Asphaltene is the *n*-heptane (C_7H_{16})-insoluble, *n*-pentane (C_5H_{12})-insoluble, toluene ($C_6H_5CH_3$)-soluble component of carbonaceous rocks (Fig. 17). Asphaltene was generally found in samples with high TOC i.e. most of the Permian rock samples shows high concentration and a few Triassic samples but with relatively less concentration. For asphaltene separation, dried samples were introduced with 5 ml of DCM such that all the organic matter in the beaker gets dissolved. After that, 150 to 200 ml of *n*-pentane was poured in it. The beakers were then covered air-tight with the aluminium foil and kept for more than one day in fume hood. The brown coloured asphaltene is found settled down at the bottom of the beakers. The *n*-pentane soluble part (i.e. maltene) was collected in another clean beaker using pipetting technique. The same process was repeated multiple times for some samples because of very high concentration of asphaltene in

them. The collected maltene was covered with aluminium foil and kept in fume hood for drying. The asphaltene left in beaker was collected and stored in 5 ml glass vials for future analysis.

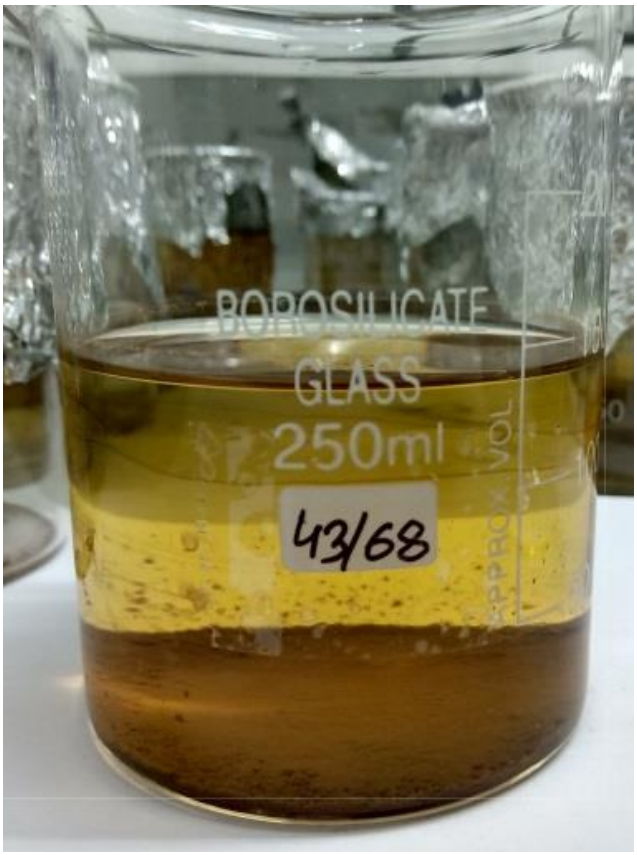

Figure 17: The asphaltene fraction settled at the bottom of the beaker and the supernatant maltene fraction.

3.2.3 FRACTIONATION USING SILICA-GEL CHROMATOGRAPHY

The dried maltene is a mixture of different class of organic compounds mainly saturated organic compounds, aromatic compounds and polar organic compounds (Fig. 18). The direct GC run of maltene may produce a highly co-eluted chromatogram. The fractionation of maltene is done to eliminate the co-elution generated by the elution of saturated and unsaturated organic compounds with the same retention time. For this, the bottom of a clean and baked (at 350°C) column was fitted and blocked with glass wool and filled with baked silica gel. The dried maltene was dissolved in a few milliliter of dichloromethane and sonicated for complete dissolution of the

dried sample in beaker. The solution was now pipetted out using a clean dropper and loaded on top of the silica gel. The column is subsequently kept for drying.

For the separation of different fractions, three different solutions were used. Firstly, hexane was used for the separation of saturated organic compounds. The volume of hexane used to completely rinse the silica gel is called dead volume. The total amount of the hexane used to separate out the saturated organic compounds was [dead volume + (3/8) dead volume + 2] ml. The extra 2 ml was added to ensure the complete separation of saturated fraction. The saturated fraction was collected in 15 ml glass vials or 100 ml clean beaker. To separate out the aromatic compounds, a solution of hexane and dichloromethane was used as an eluent in the ratio 4:1 respectively. The total volume of solution used for the unsaturated fraction is 4*dead volume. The aromatic fraction was collected in 15 ml glass vial or 100 ml clean beaker. To separate out the polar organic compounds, a solution of dichloromethane and methanol was used as an eluent in the ratio 4:1 respectively. The total volume of solution used for the polar fraction is 4*Dead Volume. The unsaturated fraction was collected in 15 ml glass vial or 100 ml clean beaker. All the fractions were kept in fume hood for drying.

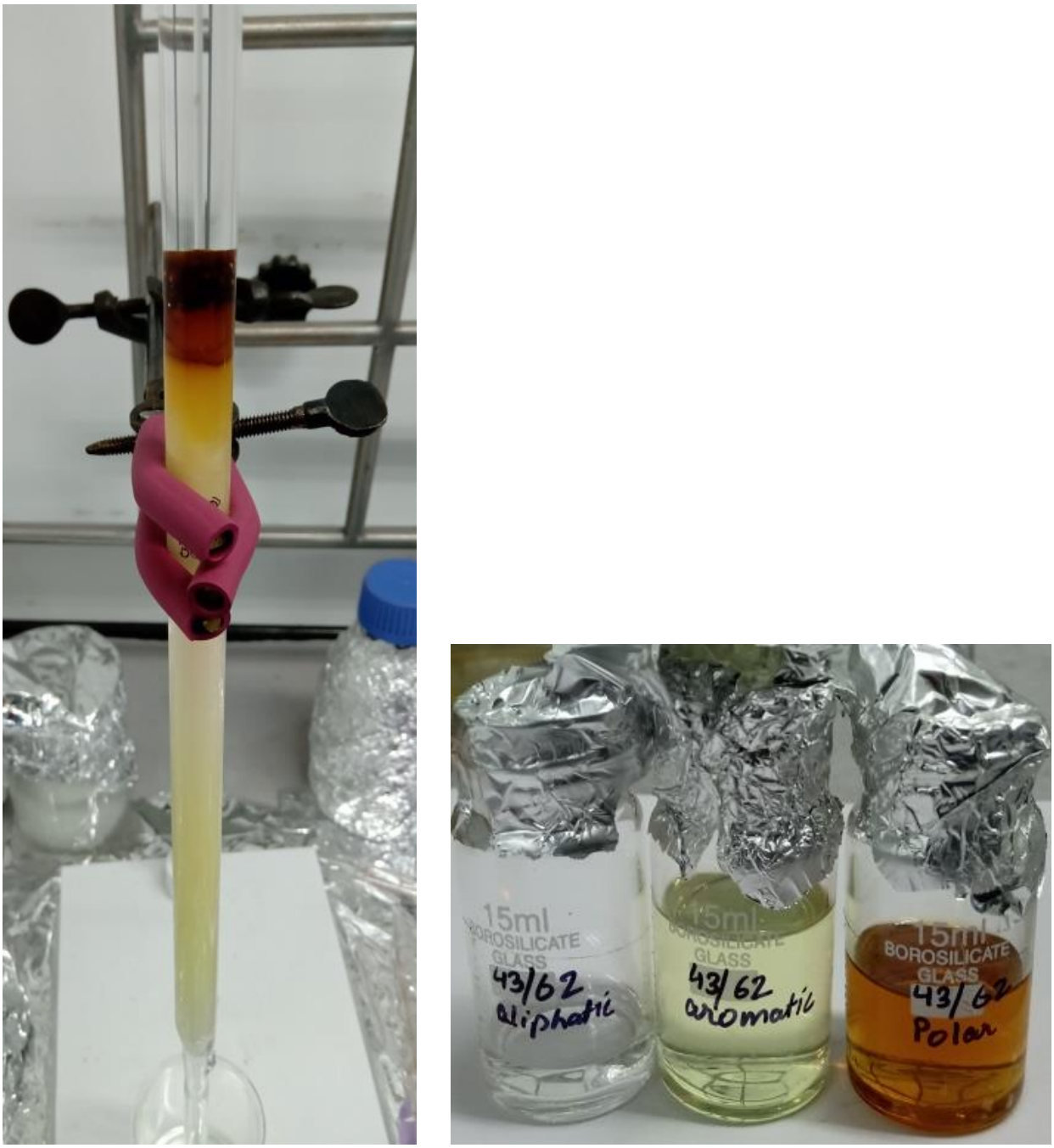

Figure 18: Photograph showing the silica gel column chromatography technique for the separation of different (saturated, aromatic and polar) hydrocarbon fractions.

3.2.4 GC-MS ANALYSIS

The fractionated aliquots were dissolved in dichloromethane and analyzed using an Agilent 5977C mass spectrometer interfaced to a 7890B gas chromatograph (Fig. 19). The samples were injected by the autosampler in pulsed splitless mode. The GC is fitted with an HP-5MS capillary column (30 m × 0.25 i.d. × 0.25 μm film thickness). Helium is used as the carrier gas with a flow rate of 1mL/min. The analysis is done in full scan mode over a mass range of 40–600 Da. The ion source operated in the electron ionization mode at 70 eV. The initial temperature of the GC oven was programmed to 40°C which remained isothermal for 5 min and then ramped to 310°C (isothermal for 5.5 min) at 4°C/min. The data was processed using Mass Hunter software and the compounds were identified by comparing the elution pattern and mass spectra from published literature. The GC-MS analysis was carried out at the PRISM lab, IISER Mohali.

Figure 19: Photograph of GC-MS facility at PRISM Lab, IISER Mohali.

CHAPTER 4

RESULTS AND DISCUSSION

The overall distribution in the saturated hydrocarbon fractions of the studied Permian, Triassic and the P/T boundary sediments comprises normal alkanes, acyclic isoprenoids, hopanes and traces of diterpenoids which are elaborately described in the subsequent sections.

The normal alkanes, observed at *m/z* 57, range from *n*-C_{16} to *n*-C_{33} and characterized by a bimodal distribution (Fig. 20). The higher chain alkanes ranging from *n*-C_{24} to *n*-C_{33} are characterized by odd carbon preference although no preference is visible in the mid or lower chain alkanes distribution. The short chain alkanes up to *n*-C_{19} are likely the products of microbial reworking, whereas the higher chain alkanes are derived from terrestrial plants, particularly the epicuticular waxes (Peters et al., 2005). The normal alkanes might be directly produced by higher plants or derivative of diagenetic alteration upon burial of organic products like acids or alcohols. The waxes play crucial role in combating desiccation through the mechanism of barrier membrane model (Andrae et al., 2019 and references therein). The model predicts that the efficiency in resisting water loss is enhanced by the increase in the concentration of the longer chain alkanes as well as narrow distribution of these longer chain homologs. Plants with the longer chain alkanes are adept in arid conditions. It is noteworthy that the normal alkanes distribution is characterized by a striking difference in the chain lengths in the Permian and Triassic samples. The Permian samples (RB/M/4X/64 and RB/M/4X/69) show higher abundances of *n*-C_{25} and *n*-C_{27} whereas the Triassic samples dominantly contain *n*-C_{27} and *n*-C_{29} (RB/M/4X/19 and RB/M/4X/47) (Fig. 21; Table 1). This shift is indicative of a shift in the vegetation across the Permian Triassic transition. The shift towards the longer chain alkanes viz. *n*-C_{27} and *n*-C_{29} likely reflects a switch from humid, swampy and coal-forming environment to growing aridity condition during the Triassic.

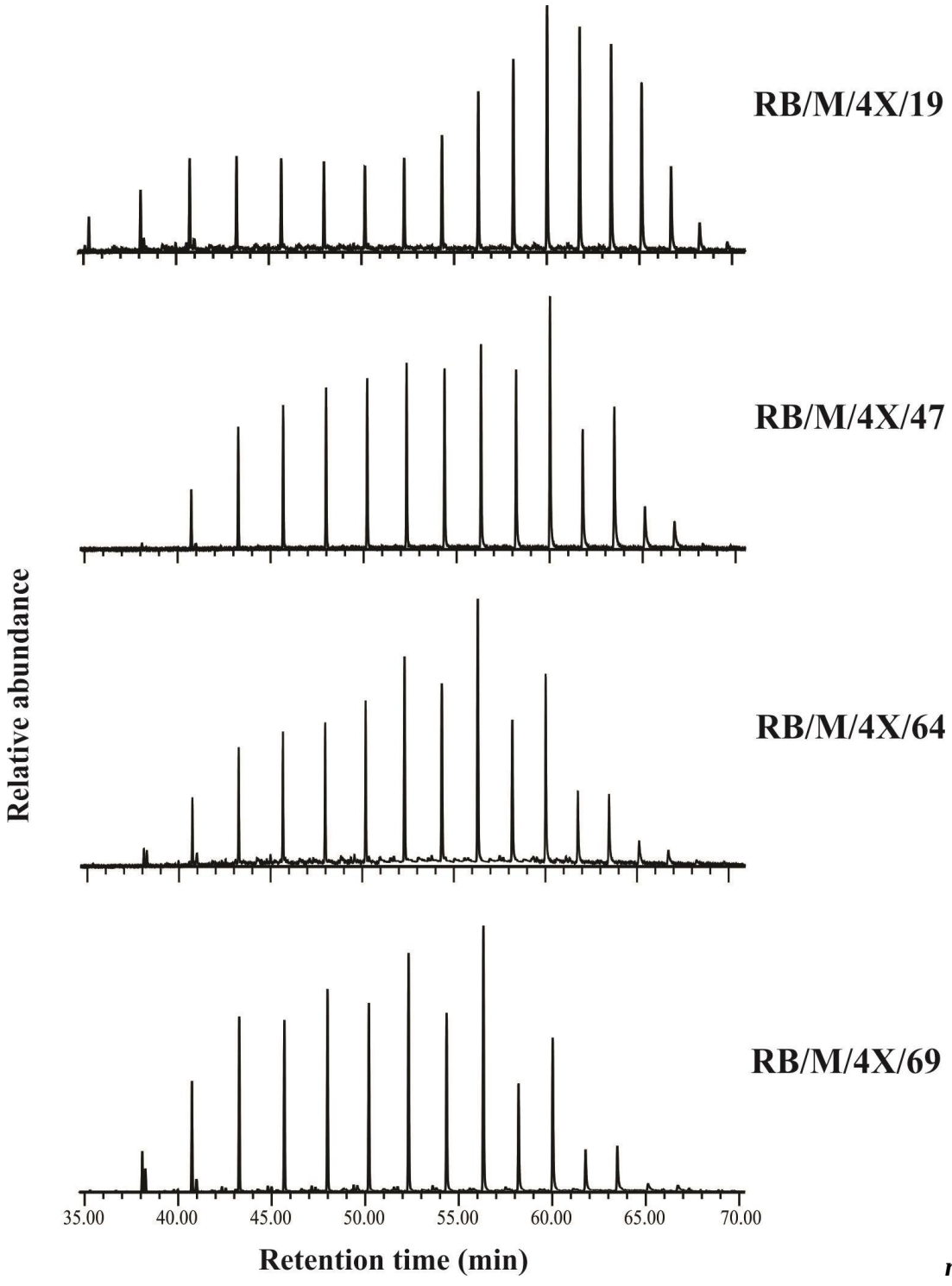

Figure 20: The normal alkanes distribution in the selected ion chromatogram at *m/z* 57 in the saturated hydrocarbon fraction of Permian (RB/M/4X/64 and RB/M/4X/69) and Triassic (RB/M/4X/47 and RB/M/4X/19) continental sediments from Raniganj sub-basin showing a shift in the dominant chain lengths.

Table 1: The ratio between mid chain *n*-alkanes (*n*-C_{23} and *n*-C_{25}) and the higher chain n-alkanes (*n*-C_{27} and *n*-C_{29}) depicting the source input in the Permian and Triassic continental sediments from Raniganj sub-basin.

Serial No.	Sample No.	Depth (m)	$(C_{23}+C_{25})/(C_{27}+C_{29})$
1	43-19	50.525	0.48
2	43-24	70.25	0.73
3	43-27	78.285	0.62
4	43-28	91.515	0.56
5	43-32	112.09	0.94
6	43-33	113.63	0.62
7	43-41	150.505	1.21
8	43-44	160.2	0.87
9	43-47	178.01	0.82
10	43-51	188.75	1.12
11	43-54	195.525	0.75
12	43-55	199.9	0.95
13	43-58	204.975	1.99
14	43-60	222	0.46
15	43-61	226	3.63
16	43-62	228.5	3.12

17	43-63	231.505	1.4
18	43-64	234.95	1.58
19	43-65	236.305	1.52
20	43-66	241.45	1.25
21	43-67	243.505	1.83
22	43-68	245.7	2.56
23	43-69	249.505	3.01

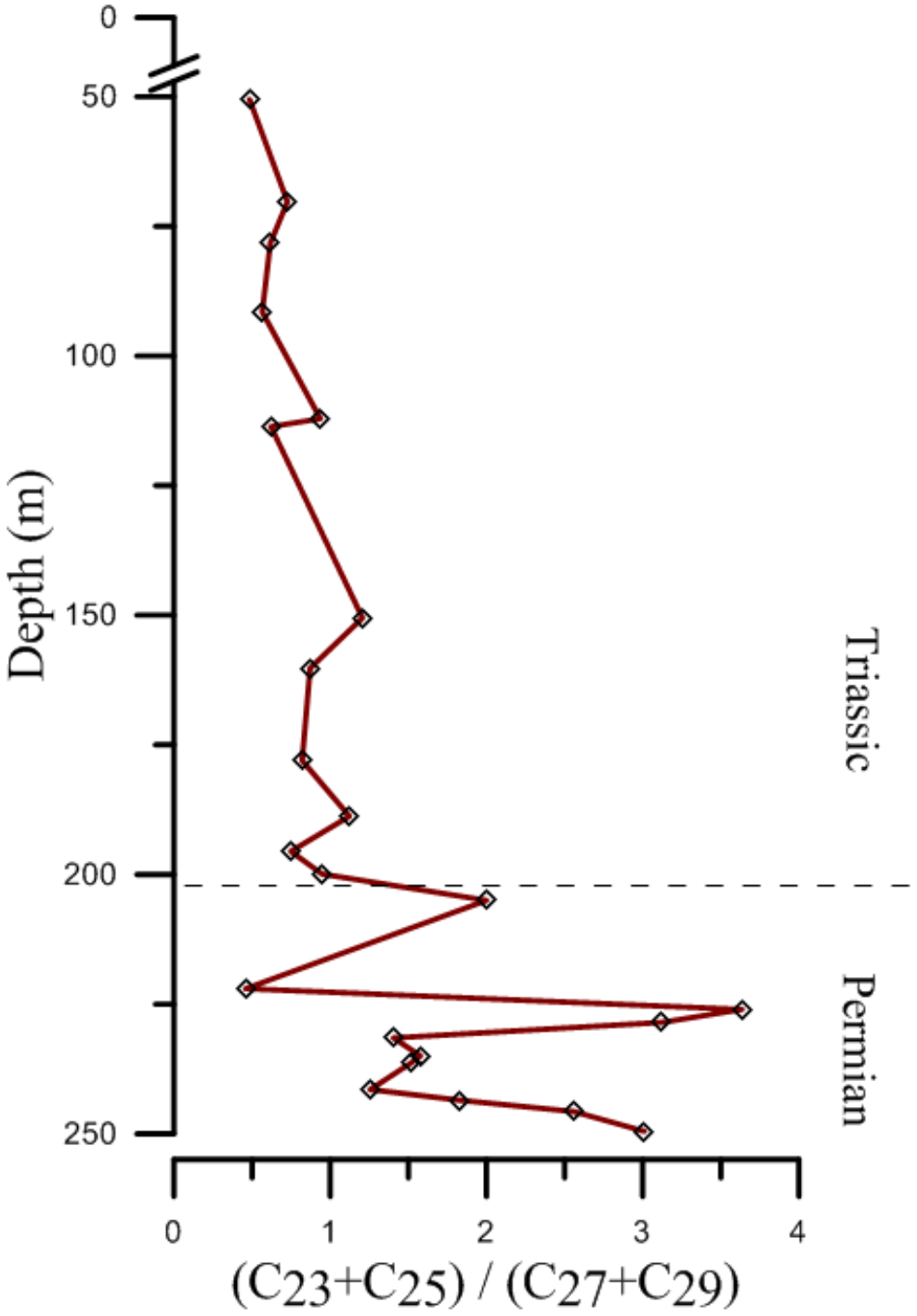

Figure 21: The shift in the *n*-alkane chain length distributions across the Permian-Triassic boundary recorded from continental sediments from Raniganj sub-basin.

The detected Pristane (Pr) and Phytane (Ph) are acyclic isoprenoids derived from the phytyl side chain of chlorophyll (Fig. 22). The side chain of chlorophyll a of photosynthetic plants and bacteriochlorophyll a and b are the more commonly known sources of these isoprenoids. Pr/Ph is generally a marker for the redox condition of the depositional environment and a high Pr/Ph ratio indicates highly oxic condition (e.g. Jiamo et al., 1990; El Diasty and Moldowan, 2012 and references therein).

In the presently studied samples, a marked shift in the redox condition can be observed based on the Pr/Ph ratio. The Permian sediments are deposited in oxic to suboxic conditions which facilitated the formation of coal in a swampy environment. However, a sharp drop in the Pr/Ph ratio is observed for the Triassic sediments which indicate a shift in the Eh condition of the depositional environment towards lower oxicity (Fig. 23; Table 2).

Table 2: Ratio of pristane/phytane recorded from continental Permo-Triassic sediments from Raniganj sub-basin

Serial no.	Sample no.	Depth (m)	Pristane/Phytane
1	43/19	50.525	0.98
2	43/24	70.25	0.83
3	43/27	78.285	1.36
4	43/28	91.515	1.12
5	43/32	112.09	1.22
6	43/41	150.505	2.14
7	43/44	160.2	0.32
8	43/51	188.75	1.04
9	43/55	199.9	0.67
10	43/58	204.975	1.70
11	43/61	226	5.16
12	43/62	228.5	5.33
13	43/63	231.505	1.50
14	43/64	234.95	1.16
15	43/65	236.305	2.19
16	43/67	243.505	2.88
17	43/68	245.7	4.69
18	43/69	249.505	1.72

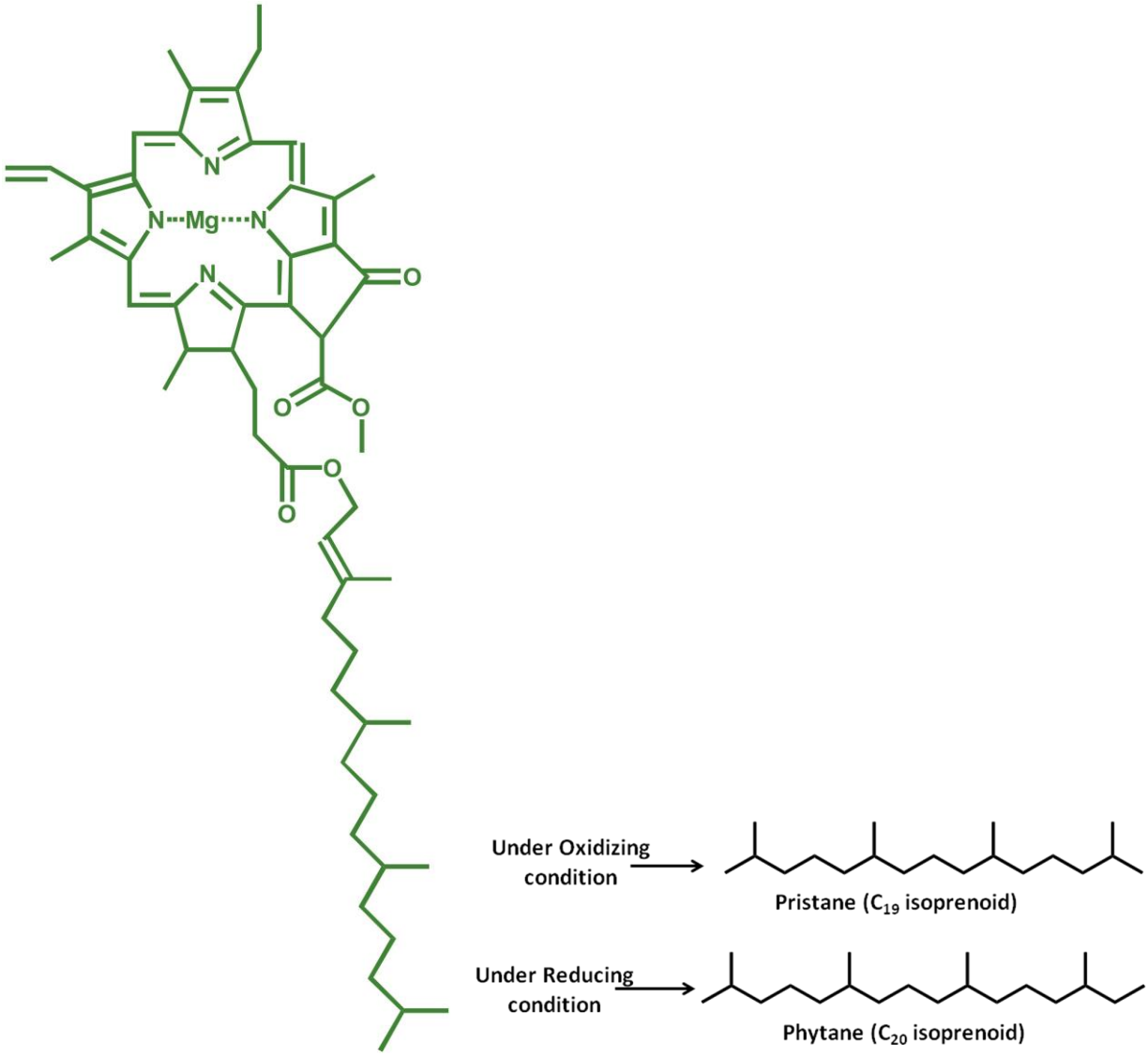

Figure 22: Structure of chlorophyll showing the phytyl chain length attached to the porphyrin ring. Pristane and phytane are diagenetically altered products of phytyl chain in oxidising and reducing conditions, respectively.

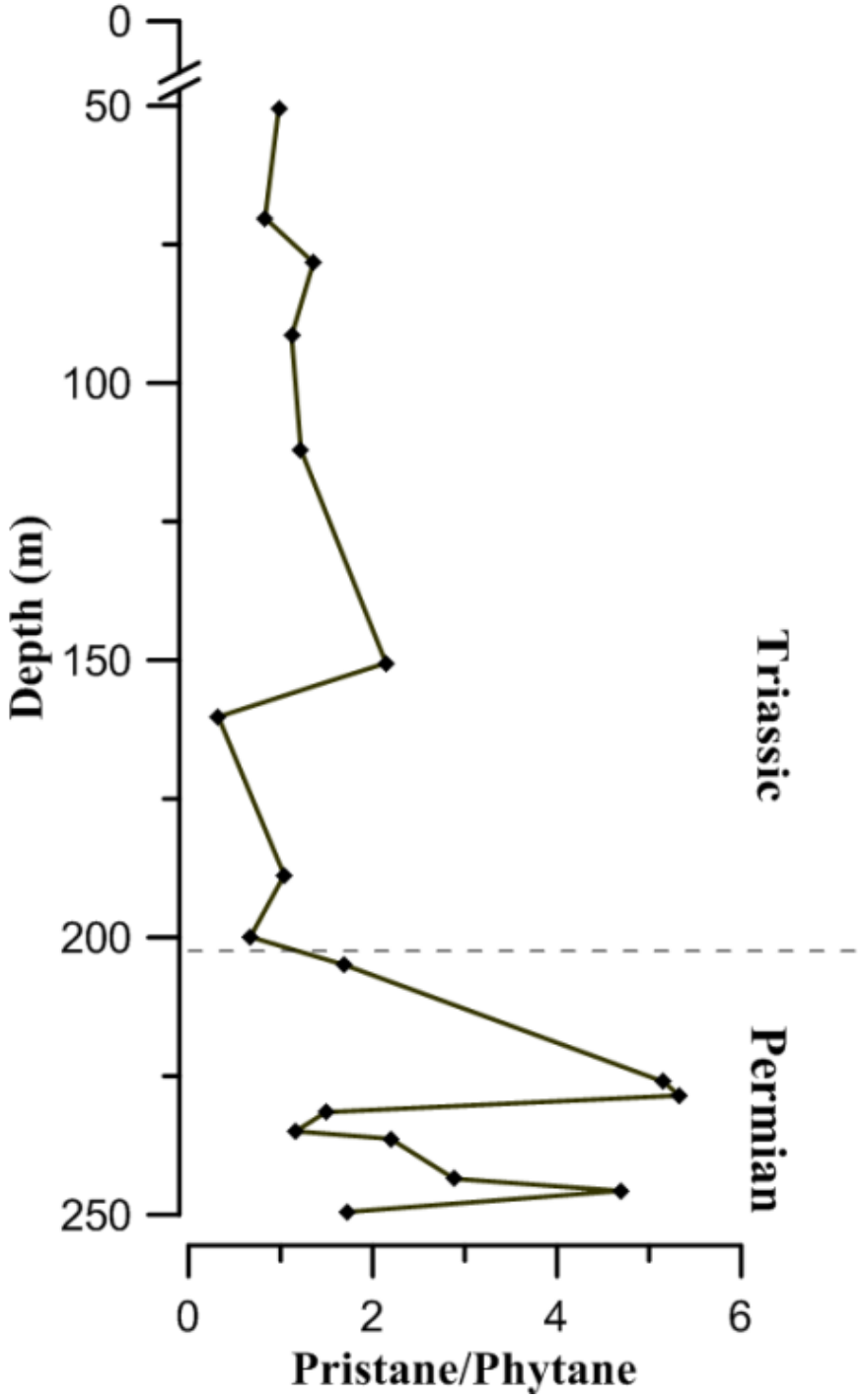

Figure 23: The shift in the pristine/phytane ratio across the Permian- Triassic boundary recorded from continental sediments from Raniganj sub-basin.

The hopanoid series in the samples comprises of C_{27}-C_{32} hopanes detected in the selected ion chromatogram at *m/z* 191(Fig. 24). 18α(H)-Trisneonorhopane (Ts) and 17α(H)-trisnorhopane (Tm) are detected. C_{29} hopane and C_{29} norhopane are also detected. Both αβ and βα (moretane) isomers are present for C_{30} hopanes. S and R stereoisomers of C_{31} αβ and C_{32} αβ homohopanes are observed; however the higher homologues are below detecting limit. The homohopanes are derivatives of functionalized hopanes i.e. with functional groups attached at C-30 hopane skeleton. In many cases, the functional group attached is D-pentose. Both Ts/Tm and moretane/hopane ratios confirm high thermal maturity (low values of the ratios) of the studied samples since Tm and moretane are thermodynamically labile and hence altered to Ts and hopane, respectively. The pentacyclic hopanoids are diagenetic alteration product of bacterial cell membranes and hence in the present context their presence indicates reworking of terrestrial plant organic remains by microbes. The hopanoids are derived from squalene and the biosynthesis occurs in the absence of free oxygen (Peters et al., 2005). It is interesting to note that the concentrations of moretane, Ts and the homohopanes markedly increased in the Permian samples. The enrichment of moretane could be due to the increased input of hopanoids from the soil bacteria (French et al., 2012). Apart from direct input of βα hopanoids which have been detected in one type of soil bacteria (French et al., 2012), the mineralogy and depositional conditions may also influence the isomerization of the terpenoids. In particular, acidic sites in clay minerals catalyze and influence stereoselectivity. Likewise, the increased abundance of Ts may be a result of high clay content with active sites. However, our result is inconsistent with the previous report of Tm being generated preferentially to Ts in oxidizing conditions. As is clearly noted, high concentrations of Ts are observed in the Permian sediments which were deposited in oxidizing depositional environment (Fig. 24).

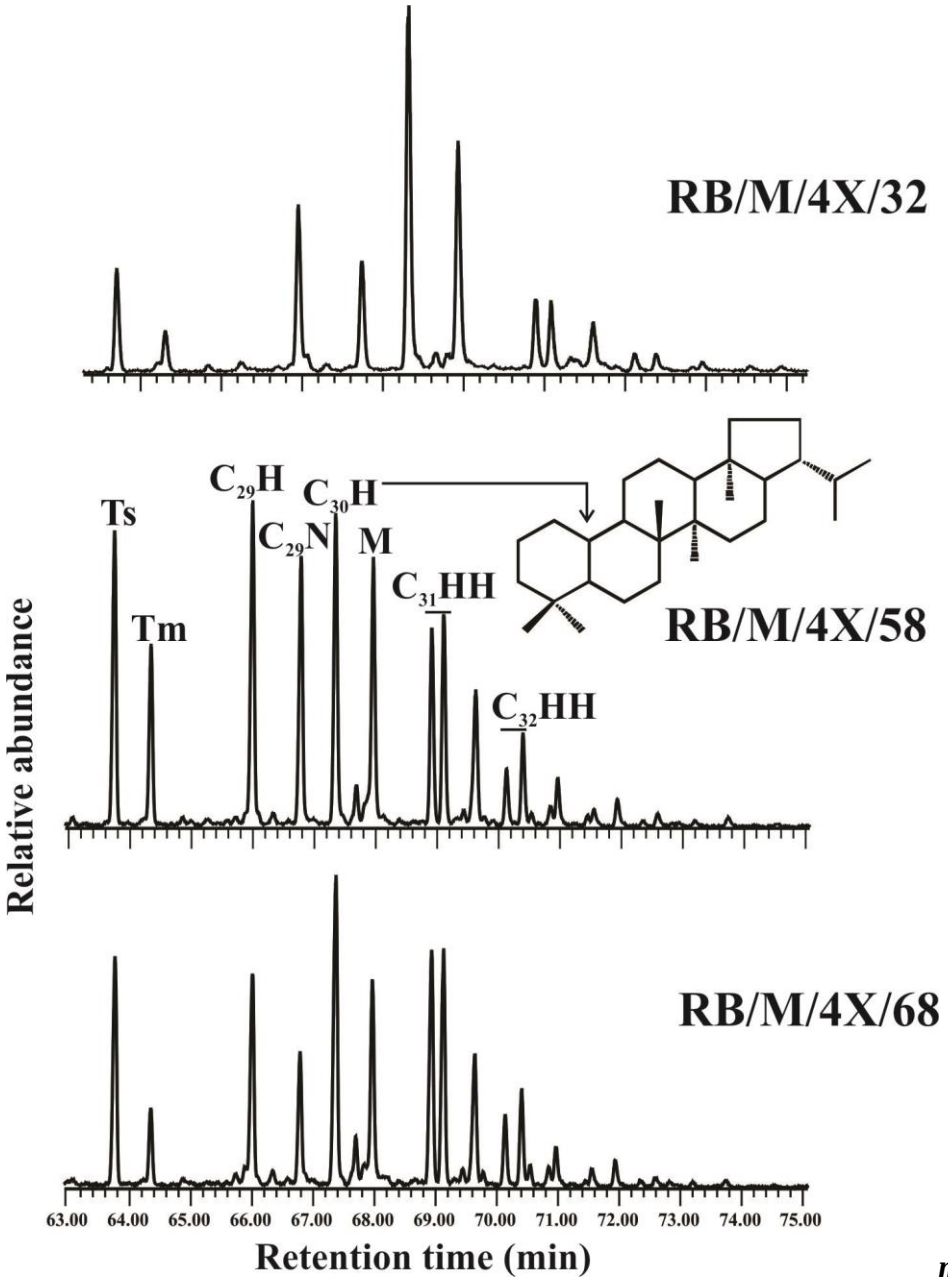

Figure 24: Selected ion chromatogram at *m/z* 191 showing the relative abundance of hopanes in the saturated hydrocarbon fraction of Permian (RB/M/4X/32), P/T boundary (RB/M/4X/58) and Triassic (RB/M/4X/68) continental sediments from Raniganj sub-basin.

A few selected diterpenoids were detected in the studied sediments at the selected ion chromatogram at *m/z* 123. 4β(H)-19-Norisopimarane, a tricyclic diterpane, was detected in low abundance in the Triassic samples detected in the selected ion chromatogram at *m/z* 233; however, a diverse variety of diterpenoids were detected in the Permian sediments viz. C_{18} norditerpane and tetracyclic diterpanes like *ent*-kaurane and 16β(H)phyllocladane in addition to 4β(H)-19-norisopimarane. Interestingly, a certain diterpenoid - *ent*-18-nor-16β(H)-kaurane recorded in the selected ion chromatogram at *m/z* 245 was detected in very high abundance in the Permian and the P/T boundary sediments; however, it is markedly absent in the Triassic sediments (Fig. 25).

The diterpenoids are largely derived from resins of terrigenous plants, conifers in particular (Otto et al., 1997). The diterpenoids are particularly distributed in gymnosperms and rarely observed in angiosperms (Otto et al., 1997); hence these are widely used from chemotaxonomic studies of past gymnosperm biota. Phyllocladane has a limited distribution as compared to the tricyclic diterpanes in the geological record. It is interesting to note that phyllocladane has been observed in conifer families such as Podocarpaceae, Taxodiaceae, Araucariaceae and Cupressaceae; however, it has not been detected in Pinaceae. On the other hand, the pimarane-type compounds are widely detected in Pinaceae and Taxodiaceae. It is noteworthy that the diterpanes reported in the present study are all derivatives of primitive conifer families which are now extinct since modern conifers had not evolved during Permian period. The lower abundance and diversity of the diterpenoids in the Triassic sediments are probably reflective of the loss in biodiversity of the gymnosperm families linked to the extinction event.

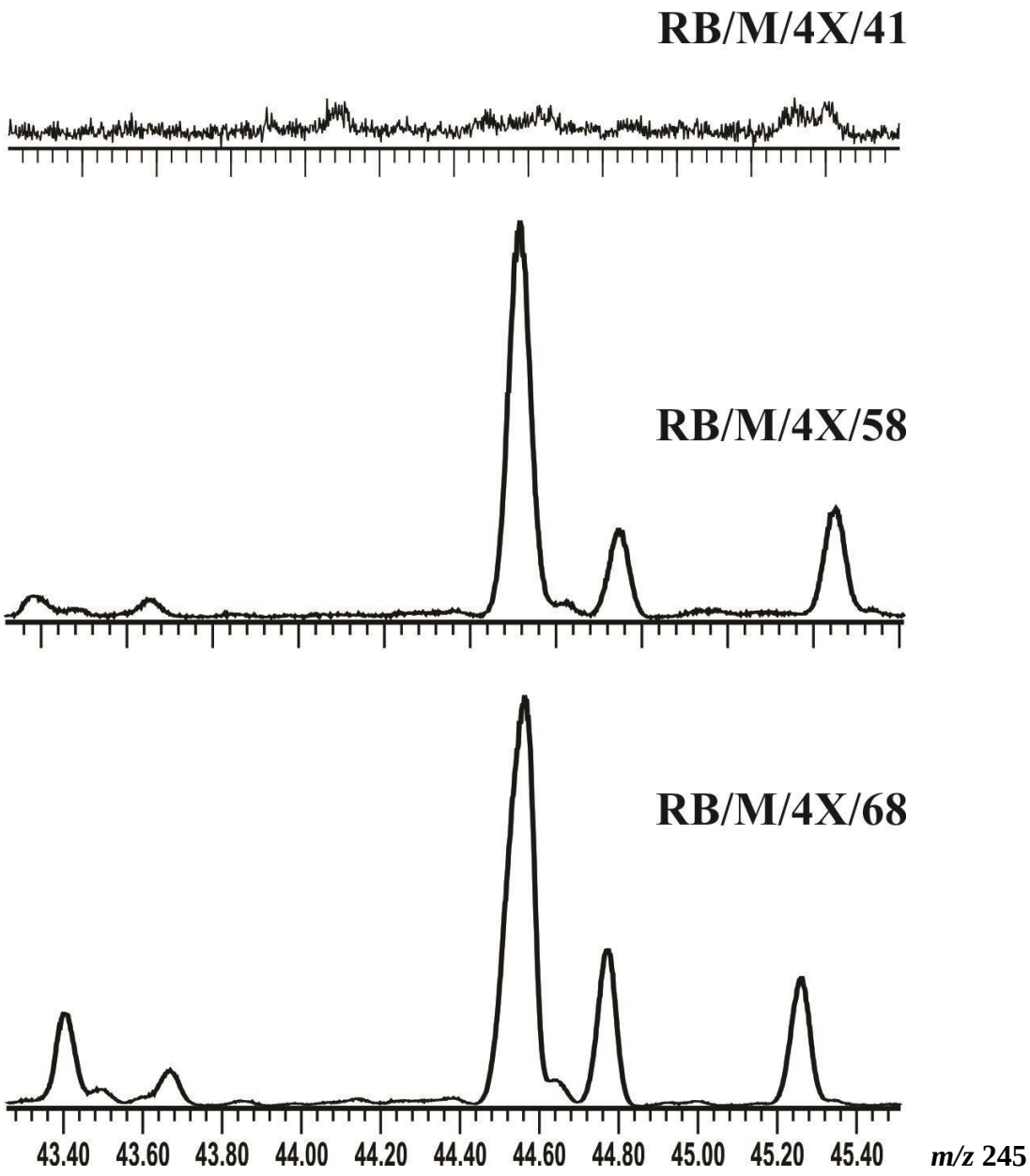

Figure 25: Selected ion chromatogram at *m/z* 245 showing the presence of *ent*-18-nor-16β(H)-kaurane in the saturated hydrocarbon fraction of Permian (RB/M/4X/68) and P/T boundary sediments (RB/M/4X/58); however, the compound is not detected in the Triassic sediment (RB/M/4X/41).

The TOC content of the Permian samples shows high values ranging from 2.09 to 51.8 (average = 12.5), whereas low values (0.41 to 0.02; average= 0.13) are observed for Triassic samples (Table 3). The $\delta^{13}C$ values shows a distinct trend during the Permian and Triassic time window with values ranges from –21.0 to –32.5‰ (mean value= –25.8‰) (Fig. 26). The $\delta^{13}C$ values remain between –21.0 to –24.0 ‰ during Permian period. However, a sharp excursion (ca. 8‰) is observed during the P-T boundary. The $\delta^{13}C$ values of Triassic period is characterized by relatively lower values ranging between –24.1 to –32.5 ‰ (average= -26.7‰). The nonparametric Mann-Whitney U test has been utilized to assess statistically significant differences between the $\delta^{13}C$ values of Permian and Triassic samples. This test is commonly employed to identify the significantly different groups with no specific distribution (McKnight and Najab, 2010). The Mann-Whitney U test for the $\delta^{13}C$ samples suggests that the Permian and Triassic population means are significantly different at the 95% confidence level.

The $\delta^{13}C$ values of terrestrial C_3 plants (Calvin cycle) typically lie between –20 to – 32 ‰ (O'Leary, 1988; Cerling et al., 1989; Boutton, 1991; Cerling et al., 1997; Basu et al., 2019), which covers the range (–21.0 to –32.5‰) reported in samples from Raniganj basin. The $\delta^{13}C$ values across P-T samples in Raniganj basin shows high variability (~ 11.5‰) with similar high fluctuations reported in the terrestrial paleosols P-T sequences in Antarctica (Graphite Peak) (Krull and Retallack, 2000) and Australia (Murrays Run bore) (Retallack and Jahren, 2008). In contrast, the $\delta^{13}C$ values of terrestrial P-T sections from Carlton Heights in Karoo Basin (South Africa) shows relatively minor fluctuations with values ranges from −22.6 (Late Permian) to −24.3 (Middle Triassic) (Faure et al., 1995). Further, the variability in the $\delta^{13}C$ values are mostly controlled by the factors enumerated below:

(i) relative differences in the organic matter (OM) sources in sedimentary rocks from multiple sources such as land derived vascular plants and nonvascular plants (e.g., aquatic macrophytes, algae) (Meyers, 2003; Badeck et al., 2005);

(ii) Shift in vegetation type can also affect the $\delta^{13}C$ values. The evergreens are more ^{13}C-enriched than deciduous plants (Brooks et al., 1997).

(iii) The change in $\delta^{13}C_{org}$ over time due to diagenetic alteration of OM alters the pristine $\delta^{13}C$ values. In the sedimentary environment diagenetic alteration of organic matter generally

result in ^{13}C-enrichment or depletion in the residual organic matter (Nadelhoffer and Fry 1988; McArthur et al., 1992; Muzuka and Hillaire-Marcel, 1999; Boström et al., 2007).

(iv) The changes in climate parameters such as moisture availability, atmospheric CO_2 concentration (pCO_2) and its carbon isotopic composition ($\delta^{13}C_{atm}$), temperature etc. (Farquahar et al., 1982; Schubert and Jahren, 2012; Diefendorf et al., 2010) can also exert control on the $\delta^{13}C$ values. The $\delta^{13}C$ values are significantly negatively correlated with the rainfall amount for C_3 plants (Kohn, 2010; Basu et al., 2019).

The absence of gradual enrichment or depletion trend observed in $\delta^{13}C$ values of P-T section in Raniganj basin suggests that $\delta^{13}C$ values of organic matter were not significantly altered during the decomposition (Jones et al. 2010; Agrawal et al., 2015). The high correlation (r= 0.5) between TOC content and $\delta^{13}C$ values across the P-T core samples also supports such a scenario. This interpretation has been further supported by high CPI values (2.3 to 1.1) of the P-T samples. The biomarker (*n*-alkane) data clearly suggests that the sources of organic matter (OM) in our investigated site are clearly dominated by terrestrial OM. Likewise, Kohn (2010) demonstrated that the $\delta^{13}C_{org}$ value of C_3 plant increases by 0.4‰ with a decrease in rainfall amount by 100 mm. Thus, we exclude climate factors as a potential factor controlling $\delta^{13}C$ variability in the P-T samples from Raniganj sub basin as the estimated precipitation changes using the observed variability (ca. 11.5‰) is too large to be explained. We contend that the shift in vegetation type is likely to have been the major factor controlling $\delta^{13}C$ values in the Raniganj basin. This possible shift in vegetation is concordant with our observation of the normal alkanes distribution showing striking difference in the chain lengths across the Permian and Triassic samples.

Table 3: The TOC and $\delta^{13}C$ values of continental Permo-Triassic sediments from Raniganj sub-basin.

Serial no.	Sample no.	Depth (m)	TOC	$\delta^{13}C$ (‰)
1	43/1	14.6	0.05	-26.9
2	43/6	21.465	0.17	-28.1
3	43/ 8	24.505	0.06	-25.1
4	43/ 9	25.8	0.08	-25.2
5	43/ 10	26.455	0.04	-25.4
6	43/ 15	39.55	0.14	-26.8
7	43/ 18	49.1	0.03	-24.7
8	43/ 19	50.525	0.13	-28.4
9	43/ 20	51.95	0.21	-29.7
10	43/ 23RED	65.655	0.02	-24.6
11	43/ 24	70.25	0.33	-32.5
12	43/ 25	73.6	0.09	-28.1
13	43/ 27	78.285	0.11	-29.5
14	43/ 28	91.515	0.12	-30.2
15	43/ 29	92.055	0.08	-28.9
16	43/ 30RED	92.85	0.03	-24.9
17	43/ 32	112.09	0.17	-30.4
18	43/ 33	113.63	0.08	-28.2
19	43/ 34	137	0.03	-24.2
20	43/ 35	139.615	0.07	-25.8
21	43/ 41	150.505	0.18	-29.8
22	43/ 44	160.2	0.18	-29.4
23	43/ 47	178.01	0.41	-29.8
24	43/ 48	181.2	0.06	-24.1
25	43/ 49	182.13	0.09	-23.3
26	43/ 50	185.305	0.04	-24.7
27	43/ 51	188.75	0.59	-28.8
28	43/ 52	190.6	0.07	-25
29	43/ 53	193.15	0.07	-26.1
30	43/ 54	195.525	0.15	-21.3
31	43/ 55	199.9	0.18	-21.3
32	43/ 57	202.6	0.06	-24.1
33	43/ 59	214.25	2.09	-22.7

34	43/ 60	222	2.24	-22.8
35	43/ 62	228.505	51.79	-23.6
36	43/ 63	231.505	3.39	-23.3
37	43/64	234.95	5.74	-23.3
38	43/ 65	236.305	7.64	-23.5
39	43/ 66	241.45	3.33	-22.7
40	43/ 67	253.505	4.65	-23
41	43/ 68	245.7	39.45	-24
42	43/ 69	249.505	4.23	-21

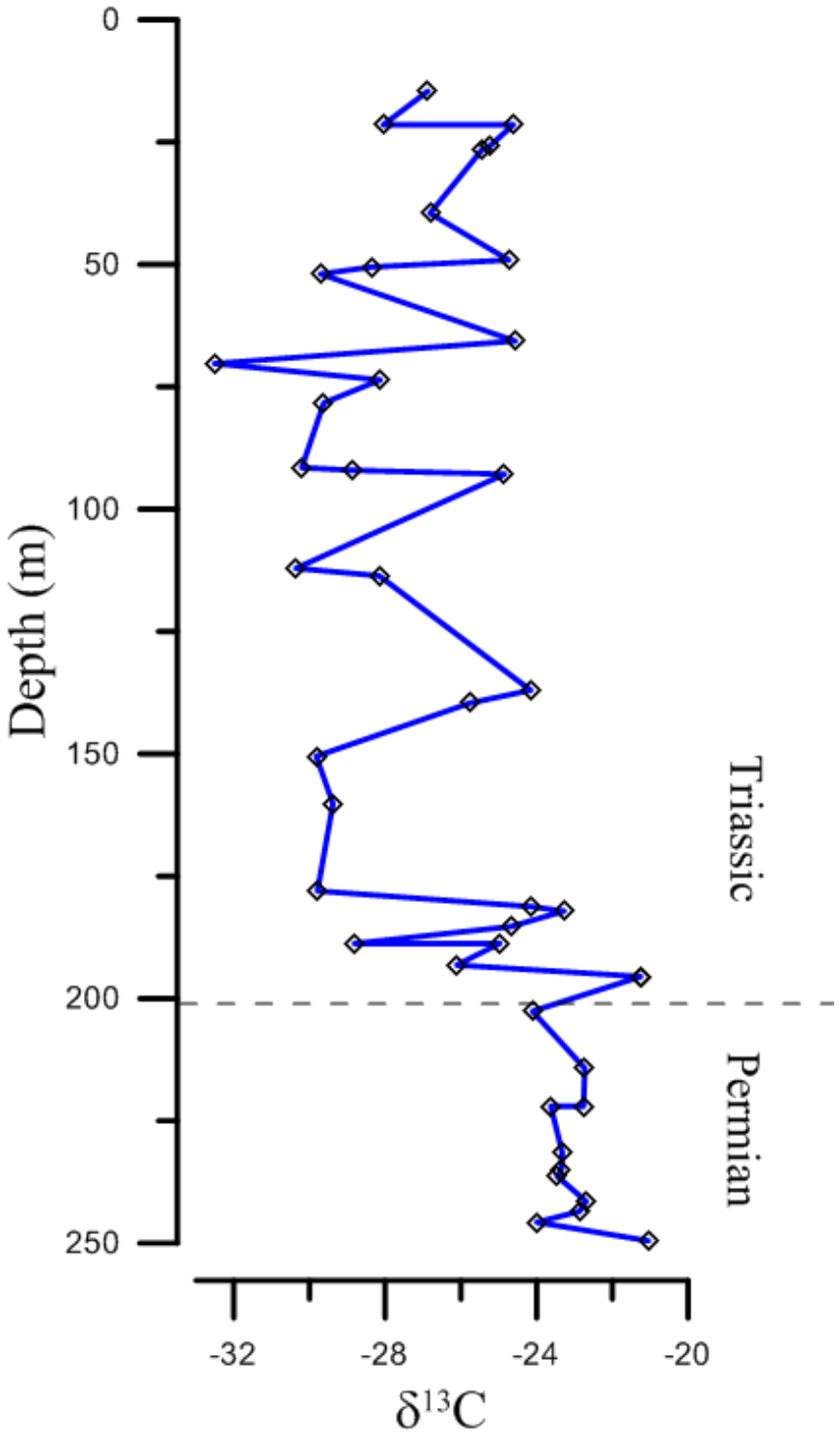

Figure 26: The carbon isotope record $\delta^{13}C_{bulk}$ showing a sharp excursion across the Permian-Triassic boundary recorded from continental sediments from Raniganj sub-basin.

CHAPTER 5

In this study, sediment samples from Permian–Triassic boundary (PTB) terrestrial sections of Raniganj basin were analyzed for biomarker and $\delta^{13}C_{bulk}$ of organic matter to understand the response of ecosystem during the end-Permian extinction event. The major findings of our investigations are as follows:

- A shift in the normal alkane chain length distribution from mid-chain *n*-alkanes in Permian to long-chain *n*-alkanes in Triassic demonstrates a turnover in the vegetation pattern.
- Stable carbon isotopic excursion of approximately 8‰ also supports abrupt vegetation shift across the P-T boundary.
- Prokaryotic inputs are evident from the presence of trisnorneohopane (Ts), trisnorhopane (Tm), C_{29} hopane, C_{30} hopane and the extended hopanes in the range of C_{31} to C_{33}.
- The Pr/Ph ratio indicates that the Permian sediments are deposited in oxic to suboxic conditions, whereas shift in the Eh condition of the depositional environment towards lower oxicity have been observed during Triassic.
- Gymnosperm input from extinct conifer biota are indicated by the presence of tricyclic diterpane 4β(H)-19-norisopimarane in the Triassic sediments and tetracyclic diterpanes *ent*-kaurane and phyllocladane in addition to 4β(H)-19-norisopimarane in the Permian sediments.

Bibliography

- Agrawal, S., Srivastava, P., Meena, N.K., Rai, S.K., Bhushan, R., Misra, D.K. and Gupta, A.K., 2015. Stable (δ 13 C and δ 15 N) isotopes and magnetic susceptibility record of late Holocene climate change from a lake profile of the northeast Himalaya. *Journal of the Geological Society of India*, *86*(6), pp.696-705.
- Algeo, T.J., Hannigan, R., Rowe, H., Brookfield, M., Baud, A., Krystyn, L. and Ellwood, B.B., 2007. Sequencing events across the Permian–Triassic boundary, Guryul Ravine (Kashmir, India). *Palaeogeography, Palaeoclimatology, Palaeoecology*, *252*(1-2), pp.328-346.
- Andrae, J., McInerney, F.A., Tibby, J., Henderson, A.C.G., Anthony Hall, P., Marshall, J.C., McGregor, G.B., Barr, C., Greenway, M., 2019. Variation in leaf wax *n*-alkane characteristics with climate in the broad-leaved paperbark (*Melaleuca quinquenervia*). *Organic Geochemistry*, doi: https://doi.org/10.1016/j.orggeochem.2019.02.004.
- Archangelsky, S., 1996. Aspects of Gondwana paleobotany: gymnosperms of the Paleozoic—Mesozoic transition. *Review of Palaeobotany and Palynology*, *90*(3-4), pp.287-302.
- Badeck, F.W., Tcherkez, G., Nogues, S., Piel, C. and Ghashghaie, J., 2005. Post-photosynthetic fractionation of stable carbon isotopes between plant organs—a widespread phenomenon. *Rapid Communications in Mass Spectrometry: An International Journal Devoted to the Rapid Dissemination of Up-to-the-Minute Research in Mass Spectrometry*, *19*(11), pp.1381-1391.
- Barnosky, A.D., Hadly, E.A., Bascompte, J., Berlow, E.L., Brown, J.H., Fortelius, M., Getz, W.M., Harte, J., Hastings, A., Marquet, P.A. and Martinez, N.D., 2012. Approaching a state shift in Earth's biosphere. *Nature*, *486*(7401), p.52.
- Basu, S., Sanyal, P., Pillai, A.A. and Ambili, A., 2019. Response of grassland ecosystem to monsoonal precipitation variability during the Mid-Late Holocene: Inferences based on molecular isotopic records from Banni grassland, western India. *PloS one*, *14*(4), p.e0212743.
- Benton, M.J. and Twitchett, R.J., 2003. How to kill (almost) all life: the end-Permian extinction event. *Trends in Ecology & Evolution*, *18*(7), pp.358-365.
- Boström, B., Comstedt, D. and Ekblad, A., 2007. Isotope fractionation and 13 C enrichment in soil profiles during the decomposition of soil organic matter. *Oecologia*, *153*(1), pp.89-98.
- Boutton, T.W., 1991. Stable carbon isotope ratios of natural materials: 2. Atmospheric, terrestrial, marine, and freshwater environments. In *Carbon isotope techniques*.
- Brocks, J.J. and Pearson, A., 2005. Building the biomarker tree of life. *Reviews in Mineralogy and Geochemistry*, *59*(1), pp.233-258.

- Brocks, J.J., Summons, R.E. and Heinrich, D.H., 2003. Sedimentary Hydrocarbons, Biomarkers for Early Life Treatise on Geochemistry. *Elsevier, Amsterdam*, *8*, p.63.
- Brooks, J.R., Flanagan, L.B., Buchmann, N. and Ehleringer, J.R., 1997. Carbon isotope composition of boreal plants: functional grouping of life forms. *Oecologia*, *110*(3), pp.301-311.
- Cao, C., Love, G.D., Hays, L.E., Wang, W., Shen, S. and Summons, R.E., 2009. Biogeochemical evidence for euxinic oceans and ecological disturbance presaging the end-Permian mass extinction event. *Earth and Planetary Science Letters*, *281*(3-4), pp.188-201.
- Cerling, T.E., Harris, J.M., MacFadden, B.J., Leakey, M.G., Quade, J., Eisenmann, V. and Ehleringer, J.R., 1997. Global vegetation change through the Miocene/Pliocene boundary. *Nature*, *389*(6647), p.153.
- Cerling, T.E., Quade, J., Wang, Y. and Bowman, J.R., 1989. Carbon isotopes in soils and palaeosols as ecology and palaeoecology indicators. *Nature*, *341*(6238), p.138.
- Chen, B., Joachimski, M.M., Shen, S., Lambert, L.L., Lai, X., Wang, X., Chen, J., Yuan, D., 2013. Permian ice volume and palaeoclimate history: Oxygen isotope proxies revisited. *Gondwana Research*, *24*, pp.77-89.
- Chen, Z.Q. and Benton, M.J., 2012. The timing and pattern of biotic recovery following the end-Permian mass extinction. *Nature Geoscience*, *5*(6), p.375.
- Cui, Y., Bercovici, A., Yu, J., Kump, L.R., Freeman, K.H., Su, S. and Vajda, V., 2017. Carbon cycle perturbation expressed in terrestrial Permian–Triassic boundary sections in South China. *Global and planetary change*, *148*, pp.272-285.
- Diefendorf, A.F., Freeman, K.H., Wing, S.L. and Graham, H.V., 2011. Production of n-alkyl lipids in living plants and implications for the geologic past. *Geochimica et Cosmochimica Acta*, *75*(23), pp.7472-7485.
- El Diasty, W.S. and Moldowan, J.M., 2012. Application of biological markers in the recognition of the geochemical characteristics of some crude oils from Abu Gharadig Basin, north Western Desert–Egypt. *Marine and Petroleum Geology*, *35*(1), pp.28-40.
- Erwin, D.H., 1994. The Permo–Triassic extinction. *Nature*, *367*(6460), p.231.
- Farquahar, G.D., Lange, S.V.C.O., Nobel, P.S., Osmond, C.B. and Ziegler, H., 1982. Encyclopedia of Plant Physiology, New Series. *12B*, *Springer-Verlag, Berlin and New York*, pp.549-587.
- Faure, K., de Wit, M.J. and Willis, J.P., 1995. Late Permian global coal hiatus linked to 13C-depleted CO2 flux into the atmosphere during the final consolidation of Pangea. *Geology*, *23*(6), pp.507-510.
- Fenton, S., Grice, K., Twitchett, R.J., Böttcher, M.E., Looy, C.V. and Nabbefeld, B., 2007. Changes in biomarker abundances and sulfur isotopes of pyrite across the

Permian–Triassic (P/Tr) Schuchert Dal section (East Greenland). *Earth and Planetary Science Letters*, *262*(1-2), pp.230-239.

- Flügel, E., 1994. Pangean shelf carbonates: controls and paleoclimatic significance of Permian and Triassic reefs. *Geological Society of America, Special Paper*, *288*, pp.247-266.
- French, K.L., Tosca, N.J., Cao, C. and Summons, R.E., 2012. Diagenetic and detrital origin of moretane anomalies through the Permian–Triassic boundary. *Geochimica et Cosmochimica Acta*, *84*, pp.104-125.
- Ghosh, P., Bhattacharya, S.K., Shukla, A.D., Shukla, P.N., Bhandari, N., Parthasarathy, G., Kunwar, A.C., 2002. Negative $\delta^{13}C$ excursion and anoxia at the Permo-Triassic boundary in the Tethys sea. *Current Science, 83*, pp.498–502.
- Ghosh, A.K., Kar, R. and Chatterjee, R., 2015. Leaf galls on Dicroidium hughesii (Feistmantel) Lele from the Triassic of India—a new record. *Alcheringa: An Australasian Journal of Palaeontology*, *39*(1), pp.92-98.
- Ghosh, N., Basu, A.R., Bhargava, O.N., Shukla, U.K., Ghatak, A., Garzione, C.N. and Ahluwalia, A.D., 2016. Catastrophic environmental transition at the Permian-Triassic Neo-Tethyan margin of Gondwanaland: Geochemical, isotopic and sedimentological evidence in the Spiti Valley, India. *Gondwana Research*, *34*, pp.324-345.
- Ghosh, S.C., 2002. The Raniganj coal basin: an example of an Indian Gondwana rift. *Sedimentary Geology*, *147*(1-2), pp.155-176.
- Grice, K., Cao, C., Love, G.D., Böttcher, M.E., Twitchett, R.J., Grosjean, E., Summons, R.E., Turgeon, S.C., Dunning, W. and Jin, Y., 2005. Photic zone euxinia during the Permian-Triassic superanoxic event. *Science*, *307*(5710), pp.706-709.
- Gupta, A., 1999. Early Permian palaeoenvironment in Damodar valley coalfields, India: an overview. *Gondwana Research*, *2*(2), pp.149-165.
- Hochuli, P.A., Hermann, E., Vigran, J.O., Bucher, H. and Weissert, H., 2010. Rapid demise and recovery of plant ecosystems across the end-Permian extinction event. *Global and Planetary Change*, *74*(3-4), pp.144-155.
- Hongfu, Y., Kexin, Z., Jinnan, T., Zunyi, Y. and Shunbao, W., 2001. The global stratotype section and point (GSSP) of the Permian-Triassic boundary. *Episodes*, *24*(2), pp.102-114.
- Jiamo, F., Guoying, S., Jiayou, X., Eglinton, G., Gowar, A.P., Rongfen, J., Shanfa, F. and Pingan, P., 1990. Application of biological markers in the assessment of paleoenvironments of Chinese non-marine sediments. *Organic Geochemistry*, *16*(4-6), pp.769-779.
- Knoll, A.H., Bambach, R.K., Canfield, D.E. and Grotzinger, J.P., 1996. Comparative Earth history and Late Permian mass extinction. *Science*, *273*(5274), pp.452-457.

- Kohn, M.J., 2010. Carbon isotope compositions of terrestrial C3 plants as indicators of (paleo) ecology and (paleo) climate. *Proceedings of the National Academy of Sciences*, *107*(46), pp.19691-19695.

- Krull, E.S. and Retallack, G.J., 2000. δ13C depth profiles from paleosols across the Permian-Triassic boundary: Evidence for methane release. *Geological Society of America Bulletin*, *112*(9), pp.1459-1472.

- Luo, G., Wang, Y., Kump, L.R., Bai, X., Algeo, T.J., Yang, H. and Xie, S., 2011. Nitrogen fixation prevailed simultaneously with the end-Permian marine mass extinction and its implications. *Geology*, *39*, pp.647-650.

- Magaritz, M., Bart, R., Baud, A. and Holser, W.T., 1988. The carbon-isotope shift at the Permian/Triassic boundary in the southern Alps is gradual. *Nature*, *331*(6154), pp.337-339.

- McArthur, J.M., Tyson, R.V., Thomson, J. and Mattey, D., 1992. Early diagenesis of marine organic matter: Alteration of the carbon isotopic composition. *Marine Geology*, *105*(1-4), pp.51-61.

- McKnight, P.E. and Najab, J., 2010. Mann-Whitney U Test. *The Corsini encyclopedia of psychology*, pp.1-1.

- McLoughlin, S., 2001. The breakup history of Gondwana and its impact on pre-Cenozoic floristic provincialism. *Australian Journal of Botany*, *49*(3), pp.271-300.

- McLoughlin, S., 2011. Glossopteris–insights into the architecture and relationships of an iconic Permian Gondwanan plant. *Journal of the Botanical Society of Bengal*, *65*(2), pp.93-106.

- Metcalfe, I. and Isozaki, Y., 2009. Current perspectives on the Permian–Triassic boundary and end-Permian mass extinction: Preface. *Journal of Asian Earth Sciences*, *36*(6), pp.407-412.

- Meyers, P.A., 2003. Applications of organic geochemistry to paleolimnological reconstructions: a summary of examples from the Laurentian Great Lakes. *Organic geochemistry*, *34*(2), pp.261-289.

- Mukhopadhyay, G., Mukhopadhyay, S.K., Roychowdhury, M. and Parui, P.K., 2010. Stratigraphic correlation between different Gondwana basins of India. *Journal of the Geological Society of India*, *76*(3), pp.251-266.

- Muzuka, A.N. and Hillaire-Marcel, C., 1999. Burial rates of organic matter along the eastern Canadian margin and stable isotope constraints on its origin and diagenetic evolution. *Marine Geology*, *160*(3-4), pp.251-270.

- Nabbefeld, B., Grice, K., Twitchett, R.J., Summons, R.E., Hays, L., Böttcher, M.E. and Asif, M., 2010. An integrated biomarker, isotopic and palaeoenvironmental study through the Late Permian event at Lusitaniadalen, Spitsbergen. *Earth and Planetary Science Letters*, *291*(1-4), pp.84-96.

- Nadelhoffer, K.J., Fry? (1988) Controls on natural nitrogen-15 and carbon-13 abundances in forest soil organic matter. *J Soil Sci52*, pp.1633-1640.
- O'Leary, M.H., 1988. Carbon isotopes in photosynthesis. *Bioscience*, *38*(5), pp.328-336.
- Peters, K.E., Walters, C.C. and Moldowan, J.M., 2005. *The Biomarker Guide: Volume 1, Biomarkers and Isotopes in the Environment and Human History* . Cambridge University Press, Cambridge, UK.
- Peters, K.E., Walters, C.C. and Moldowan, J.M., 2005. *The Biomarker Guide: Volume 2, Biomarkers and isotopes in petroleum systems and earth history*. Cambridge University Press. Cambridge, UK.
- Peters, S.E., 2008. Environmental determinants of extinction selectivity in the fossil record. *Nature*, *454*(7204), p.626.
- Raup, D.M. and Sepkoski, J.J., 1982. Mass extinctions in the marine fossil record. *Science*, *215*(4539), pp.1501-1503.
- Retallack, G.J. and Jahren, A.H., 2008. Methane release from igneous intrusion of coal during Late Permian extinction events. *The Journal of Geology*, *116*(1), pp.1-20.
- Retallack, G.J., Veevers, J.J. and Morante, R., 1996. Global coal gap between Permian–Triassic extinction and Middle Triassic recovery of peat-forming plants. *Geological Society of America Bulletin*, *108*(2), pp.195-207.
- Sarkar, A., Yoshioka, H., Ebihara, M. and Naraoka, H., 2003. Geochemical and organic carbon isotope studies across the continental Permo–Triassic boundary of Raniganj Basin, eastern India. *Palaeogeography, Palaeoclimatology, Palaeoecology*, *191*(1), pp.1-14.
- Schubert, B.A. and Jahren, A.H., 2012. The effect of atmospheric CO2 concentration on carbon isotope fractionation in C3 land plants. *Geochimica et Cosmochimica Acta*, *96*, pp.29-43.
- Schwab, V. and Spangenberg, J.E., 2004. Organic geochemistry across the Permian–Triassic transition at the Idrijca valley, western Slovenia. *Applied geochemistry*, *19*(1), pp.55-72.
- Sepkoski, J.J., 1984. A kinetic model of Phanerozoic taxonomic diversity. III. Post-Paleozoic families and mass extinctions. *Paleobiology*, *10*(2), pp.246-267.
- Shen, S.Z., Crowley, J.L., Wang, Y., Bowring, S.A., Erwin, D.H., Sadler, P.M., Cao, C.Q., Rothman, D.H., Henderson, C.M., Ramezani, J. and Zhang, H., 2011. Calibrating the end-Permian mass extinction. *Science*, *334*(6061), pp.1367-1372.
- Shen, S.Z., Crowley, J.L., Wang, Y., Bowring, S.A., Erwin, D.H., Sadler, P.M., Cao, C.Q., Rothman, D.H., Henderson, C.M., Ramezani, J. and Zhang, H., 2011. Calibrating the end-Permian mass extinction. *Science*, *334*(6061), pp.1367-1372.
- Song, H., Wignall, P.B., Tong, J. and Yin, H., 2013. Two pulses of extinction during the Permian–Triassic crisis. *Nature Geoscience*, *6*(1), p.52.

- Svensen, H., Planke, S., Polozov, A.G., Schmidbauer, N., Corfu, F., Podladchikov, Y.Y. and Jamtveit, B., 2009. Siberian gas venting and the end-Permian environmental crisis. *Earth and Planetary Science Letters*, *277*(3-4), pp.490-500.
- Tewari, R., Pandita, S.K., McLoughlin, S., Agnihotri, D., Pillai, S.S., Singh, V., Kumar, K. and Bhat, G.D., 2015. The Permian–Triassic palynological transition in the Guryul Ravine section, Kashmir, India: implications for Tethyan–Gondwanan correlations. *Earth-Science Reviews*, *149*, pp.53-66.
- Twitchett, R.J., 2007. The Lilliput effect in the aftermath of the end-Permian extinction event. *Palaeogeography, Palaeoclimatology, Palaeoecology*, *252*(1-2), pp.132-144.
- Ward, P.D., Montgomery, D.R. and Smith, R., 2000. Altered river morphology in South Africa related to the Permian-Triassic extinction. *Science*, *289*(5485), pp.1740-1743.
- Wignall, P.B. and Hallam, A., 1992. Anoxia as a cause of the Permian/Triassic mass extinction: facies evidence from northern Italy and the western United States. *Palaeogeography, Palaeoclimatology, Palaeoecology*, *93*(1-2), pp.21-46.
- Wignall, P.B. and Twitchett, R.J., 1996. Oceanic anoxia and the end Permian mass extinction. *Science*, *272*(5265), pp.1155-1158.

APPENDIX

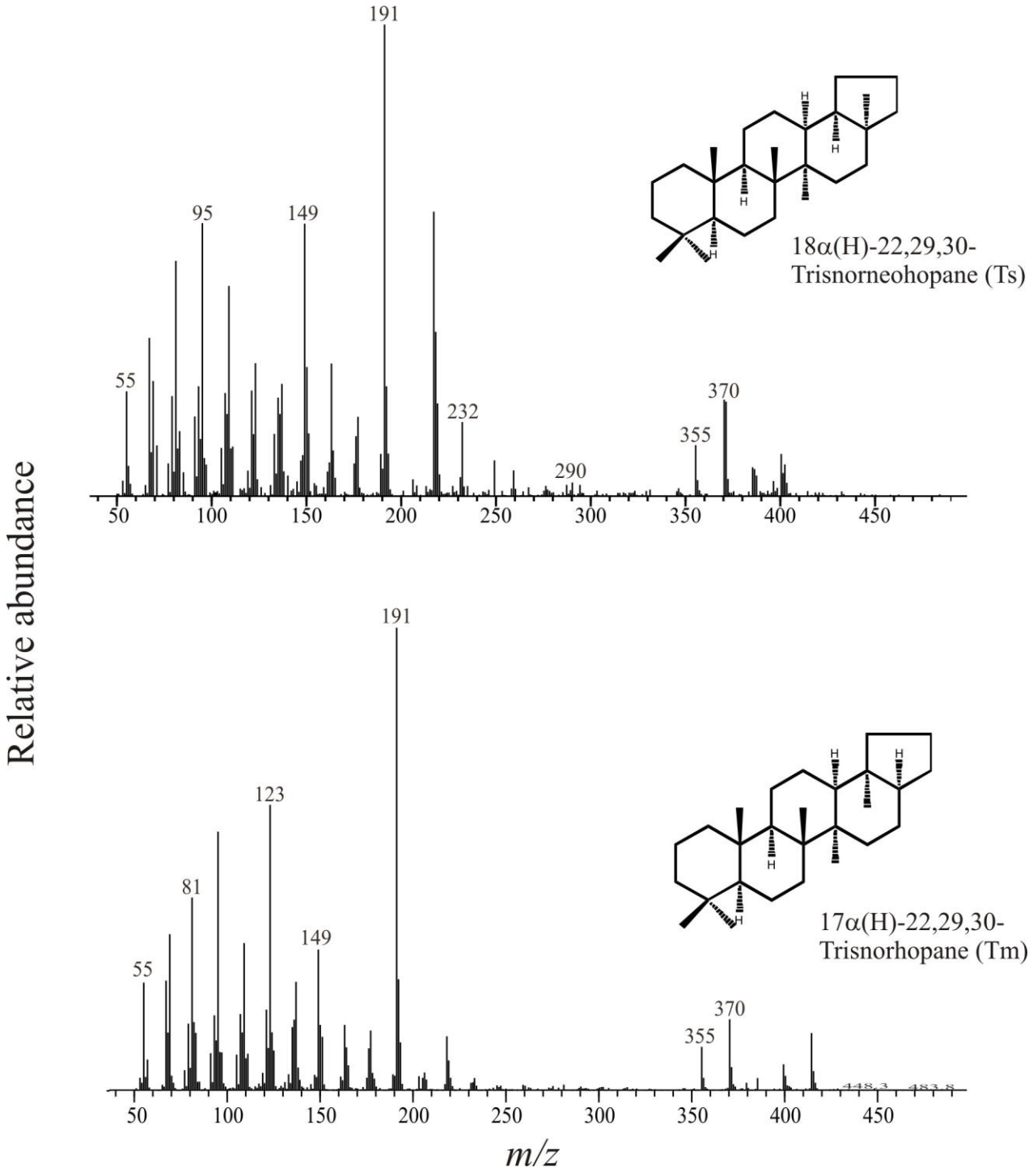
Relative abundance
191
95
149
55
232
290
355
370
18α(H)-22,29,30-
Trisnorneohopane (Ts)
191
123
81
149
55
355
370
17α(H)-22,29,30-
Trisnorhopane (Tm)
50
100
150
200
250
300
350
400
450
m/z

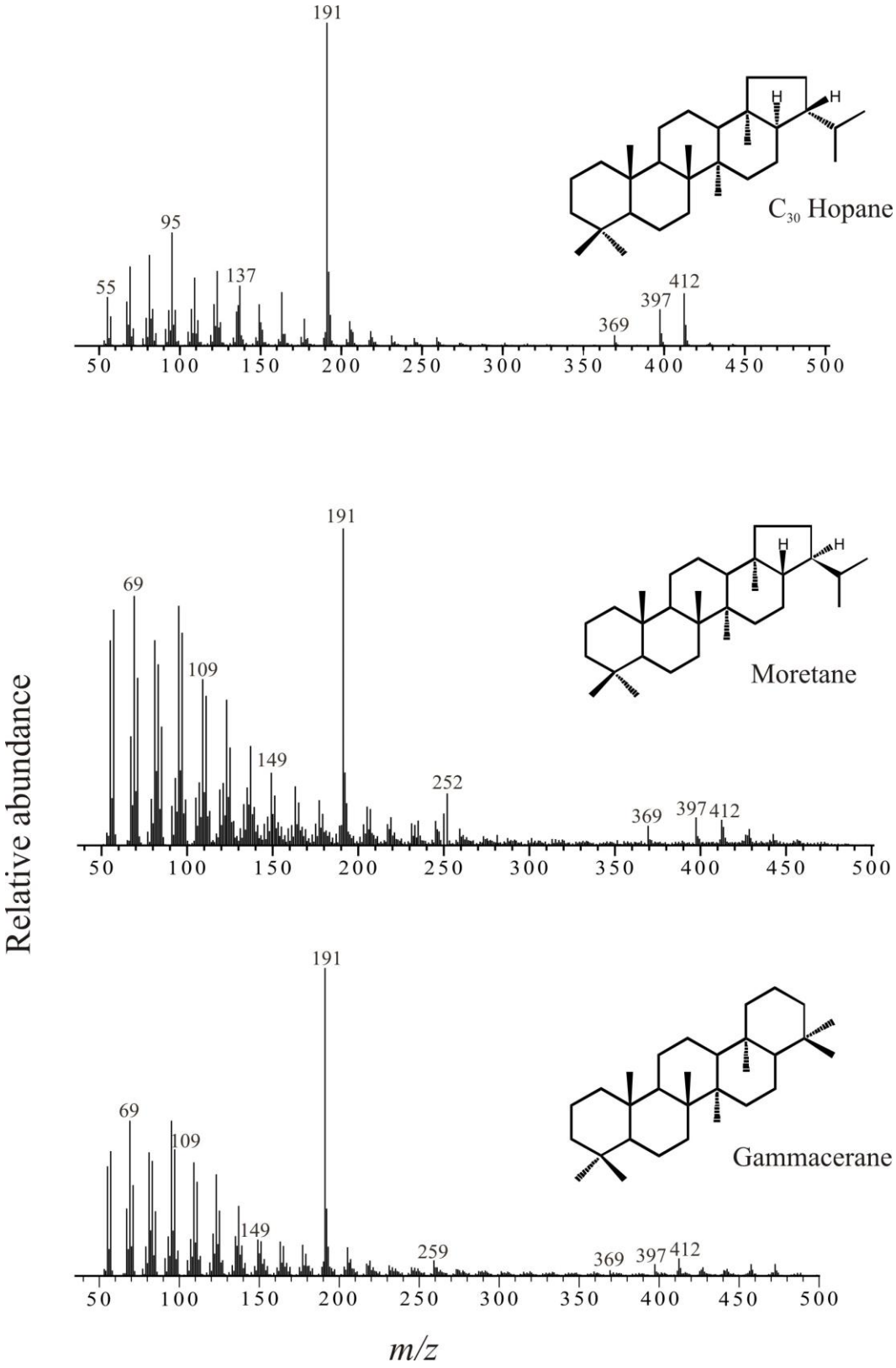
191
95
55
137
412
397
369
50 100 150 200 250 300 350 400 450 500
C30 Hopane
191
69
109
149
252
369
397
412
50 100 150 200 250 300 350 400 450 500
Moretane
191
69
109
149
259
369
397
412
50 100 150 200 250 300 350 400 450 500
Gammacerane
Relative abundance
m/z

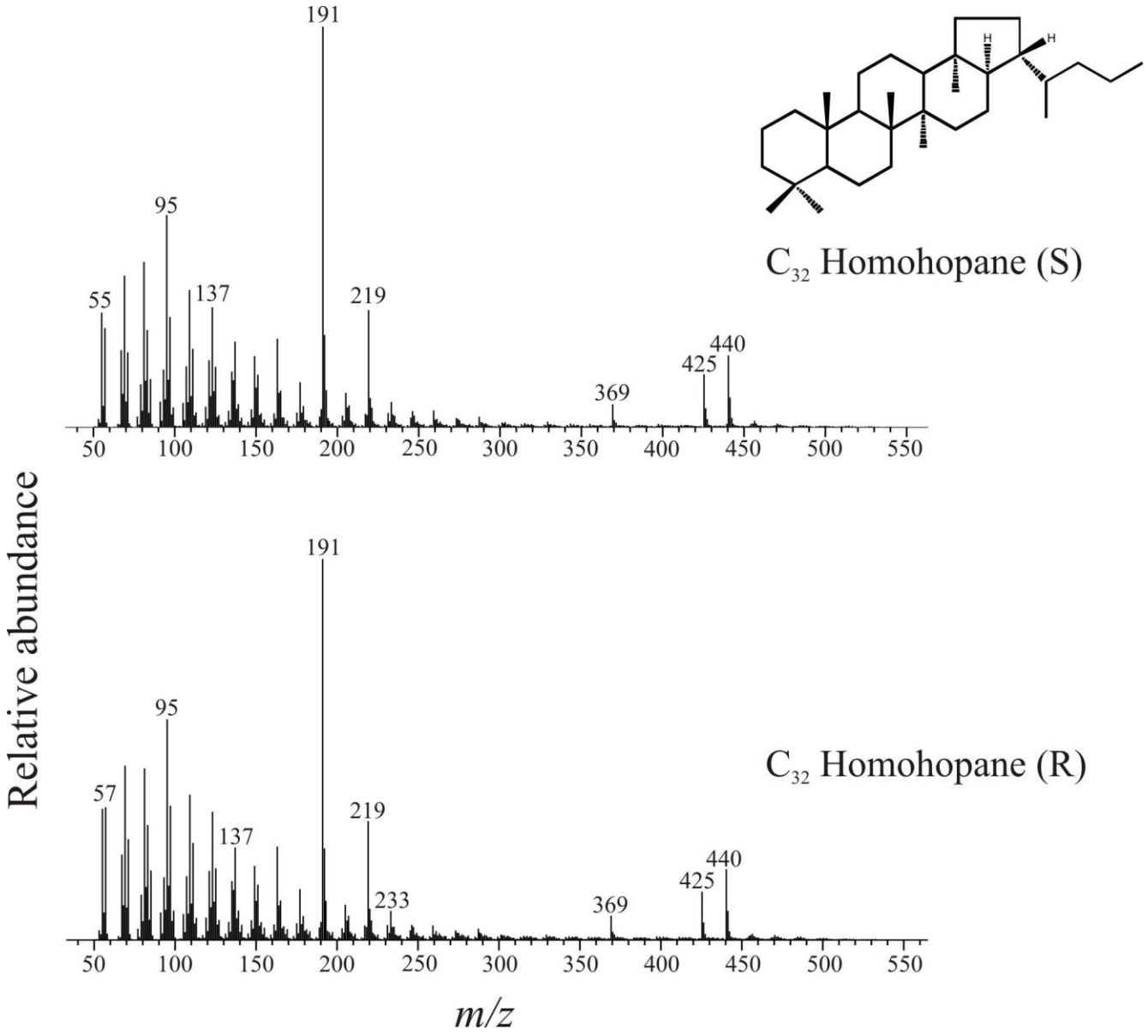
191
95
55
137
219
369
425
440
C32 Homohopane (S)
191
95
57
137
219
233
369
425
440
C32 Homohopane (R)
Relative abundance
m/z